Regional Studies in Marine Science 65 (2023) 103086

Contents lists available at ScienceDirect

Regional Studies in Marine Science

journal homepage: www.elsevier.com/locate/rsma

A risk assessment of marine plastics in coastal waters of a small island: Lessons from Ambon Island, eastern Indonesia

Gerry Giliant Salamena [a,b,c,d,*], Scott F. Heron [a,b], Peter V. Ridd [e], James C. Whinney [b]

[a] Physical Sciences, College of Science and Engineering, James Cook University, Townsville, QLD, 4811, Australia
[b] Marine Geophysics Laboratory, College of Science and Engineering, James Cook University, Townsville, QLD, 4811, Australia
[c] Marine Physics Division at Centre for Deep-Sea Research (CDSR) of National Research and Innovation Agency (BRIN) of Indonesian Government (Pusat Riset Laut Dalam – BRIN), Indonesia
[d] Centre for Collaborative Research on Aquatic Ecosystem in Eastern Indonesia (Pusat Kolaboratif Riset Ekosistem Perairan Indonesia Timur), Indonesia
[e] 34 Mango Avenue, Mundingburra, Townsville, QLD, 4812, Australia

ARTICLE INFO

Article history:
Received 30 March 2023
Received in revised form 10 June 2023
Accepted 29 June 2023
Available online 5 July 2023

Keywords:
Risk assessment of marine plastic accumulation in the Indonesian Coral Triangle region
Flushing time
Simple flushing models
Ambon Bay

ABSTRACT

This study provides the first implementation of environmental risk assessment (ERA) regarding marine plastic accumulation (environmental threat) in the water body of small islands in the Indonesian Coral Triangle region (a case study in Ambon Bay of Ambon Island). Ambon Bay is a tropical fjord system with outer Ambon Bay (OAB) separated from inner Ambon Bay (IAB) by a shallow sill. The emphasis of ERA was to combine coastal demography determining the probability of occurrence of the threat and flushing capacity of Ambon Bay determining the vulnerability of the system to the threat to evaluate risk during the peak rainfall season (easterly monsoon, June–August). Supplementarily, ERA considered the coral ecosystem in the bay contributing to the vulnerability parameter. This study only calculated flushing time (τ) of OAB due to available information on IAB flushing, and used three simple flushing models: 1D numerical advection–diffusion, salt-exchange and land–ocean interaction in coastal zone (LOICZ) models. The flushing time of the entire OAB was found to be 1–1.5 weeks. Inshore OAB was found to be flushed within 1.5–2 weeks while τ of mid OAB was 1–1.5 weeks. The flushing time of offshore OAB was $\leq$1 week. Regarding the ERA implementation, the probability of occurrence of marine plastics was very high in IAB and inshore OAB (linked to dense-populated areas) compared to in mid and offshore OAB (i.e. moderate-to-low, where sparsely population areas are located). It was also true for the vulnerability of Ambon Bay to marine plastic accumulation that was found to be high in IAB and inshore OAB, linked to slower flushing in these locations than in mid and offshore OAB, located close to the open ocean. Combining this, IAB and inshore OAB showed a high risk of marine plastic contamination than mid and offshore OAB. The knowledge of ERA regarding marine plastic accumulation presented here is informative for other embayments in Indonesia's Coral Triangle region due to their similarity to Ambon Bay in shape and demographic aspects.

1. Introduction

Marine plastics have recently emerged to be a global environmental issue. The rapid increase in the global production of plastics from 1954 (1.7 million tons) to 2014 (311 million tons) has subsequently increased the quantity of plastics entering the marine environment, whether by accident, or intentionally, worldwide (Jambeck et al., 2015; National Research Council, 1975; PlasticEurope, 2015). Due to the durability of plastics, spanning years to centuries, this increased amount of plastics in the marine environment has threatened marine life worldwide. For example, macroplastics (size: >5 mm) in the ocean such as fishing gears have been reported to degrade corals globally (Good et al., 2010; Hoeksema and Hermanto, 2018; Sheehan et al., 2017). Microplastics (size: <5 mm) have also been reported to be harmful for the coral ingestion system (Connors, 2017). Besides corals, marine wildlife (mammals, reptiles and fish) have also been affected by microplastics particularly on their digestive system increasing the likelihood of their mortality (Boerger et al., 2010; Choy and Drazen, 2013; de Stephanis et al., 2013; Wilcox et al., 2018).

An environmental risk assessment (ERA) is an effective management tool to evaluate the potential of adverse ecological impacts resulted from environmental threats (some authors called

* Corresponding author at: Marine Physics Division at Centre for Deep-Sea Research (CDSR) of National Research and Innovation Agency (BRIN) of Indonesian Government (Pusat Riset Laut Dalam – BRIN), Indonesia.
E-mail address: gerry.salamena@my.jcu.edu.au (G.G. Salamena).

https://doi.org/10.1016/j.rsma.2023.103086
2352-4855/

'hazards') typically linked to human activities (e.g. chemical threats: toxic, hazardous or dangerous substances; physical threats: habitat destruction; biological threats: introduced invasive species), and hence, implementing ERA is of interest to decision-making regarding threat management (Gómez et al., 2015; Hope, 2006; Mazarrasa et al., 2019). Here, the definition of risk is the result of (i) the threat probability and (ii) its consequences and thus, risk theoretically is a function of these two aspects (Birkmann, 2007). The consequences aspect has recently been interpreted to be due to the intrinsic characteristic of the environment towards the threats (the vulnerability component) and the effects of the threats to the environment (the consequences component) (Gómez et al., 2015). Building upon this concept, ERA provides information on (i) the nature and magnitude of environmental threats via the quantification of *probability* of occurrence of the threats; (ii) *vulnerability* of the environment to the threats indicating the characteristics of the environment that has the potential to be harmed; and (iii) *consequences* derived from the threats (e.g. environmentally or socially) (Gómez et al., 2014, 2015; Mazarrasa et al., 2019). Hence, the quantification of risk is obtained from the multiplication of these three components (Gómez et al., 2015; Mazarrasa et al., 2019). Due to its effectiveness, ERA has been widely implemented to environmental threats in marine ecosystems such as chemical pollutants (Gómez et al., 2015), dredging (Gómez et al., 2014; Suedel et al., 2008) and marine plastics (Mazarrasa et al., 2019).

Regarding the ERA implementation to marine plastic accumulation in the water body of a marine system with *consequences* already been above-highlighted as hazardous substances to marine life, the ERA component of *probability* of occurrence is typically linked to the nearby human population density; densely-populated areas commonly discharge higher amount of plastics to the marine environment than sparsely-populated areas (Fok and Cheung, 2015; Mahoney, 2017; Suyadi and Manullang, 2020). Meanwhile, the ERA component of *vulnerability* for plastic accumulation in the water body is a function of the time that marine plastics stay within a system (Bakir et al., 2014; Critchell and Lambrechts, 2016; Gómez et al., 2014, 2015; Mahoney, 2017; Vegter et al., 2014). Assessing this *vulnerability* is commonly considered using flushing time; i.e., how long water parcels reside within the marine environment (Andutta et al., 2014, 2013; Salamena et al., 2016; Wang et al., 2007). For example, marine waters with long flushing times are more likely to experience accumulation of marine plastics (e.g. isolated waters, ocean gyres) (Law et al., 2010; Mahoney, 2017). Flushing time can be estimated using analytical and numerical approaches. The analytical approaches of estimating flushing time typically consider the ratio between the spatial features (e.g. volume, depth) of a water body and the total exchange rate driven by a long-term average condition of density gradient (Andutta et al., 2014; Wang et al., 2007). In contrast, the flushing time calculation using numerical approaches is undertaken by firstly modeling water transport, considering the details of ocean circulation (i.e. baroclinic and diffusion processes) and then using the modeled water transport to determine how long virtual tracer particles remain within the water body (Andutta et al., 2013; Mao and Ridd, 2015; Salamena et al., 2016; Wang et al., 2007).

Indonesia is the world's second largest contributor of marine plastics (0.48–1.29 million tons, annually; Jambeck et al., 2015). This status is driven by increased population and, more recently, increased income and consumptive behavior combined with poor waste management systems (Jambeck et al., 2015; Ocean Conservancy, 2017; World Bank Group, 2018). Densely-populated areas (i.e. the nation's major cities located in large islands: $>$ 100,000 km^2) have been the primary contributors of marine plastics for decades; however, coastal urban areas in remotely small islands (ca. 2000 km^2 or less) have recently emerged due to development driven by human migration, economic activities and tourism (Akhir, 2018; Hermawan et al., 2017; Kakisina et al., 2015; Lebreton et al., 2017; Uneputty and Evans, 1997a). These emerging coastal urban areas have significant potential for discharging plastics into Indonesian waters in the coming years.

Impacts from marine plastics originating from urban areas of small islands in Indonesia are likely to be more significant than those found in the nation's major islands as most of these small islands are located in the eastern Indonesia that is part of the Coral Triangle, the world's marine diversity hotspot (Veron et al., 2009, 2011). Ecological impacts can include the decline in coral diversity due to plastic-caused mortality (Edinger et al., 2000; Uneputty and Evans, 1997b; Willoughby et al., 1997) and the mortality of marine megafauna (e.g. turtles, dolphins) and reef fish living in coral reefs (Broderick et al., 2015; Bugoni et al., 2001; Critchell and Hoogenboom, 2018; Panti et al., 2019; Vélez-Rubio et al., 2013). These ecological impacts lead to subsequent socio-economic impacts. For instance, degraded marine ecosystems due to marine plastics, such as polluted beaches and degraded coral reefs, can negatively affect tourism and fisheries in this region, causing the loss of income or jobs (UN Environment, 2017).

Despite the potential threats of marine plastics in the Indonesian small islands, ERA has not been implemented in this region (Suyadi and Manullang, 2020). One major hindrance is related to the quantification of the ERA component of *vulnerability* of the coastal waters of these small islands to marine plastics linked to the insufficient information on flushing time. Oceanographic data that underpin the flushing time calculation are limited in these islands primarily driven by two reasons: (i) the remote location of these islands (Purba et al., 2018); and (ii) rapid coastal development in the Indonesian large islands. Massive coastal development (i.e. reclamation, port constructions) in Indonesian larger islands commonly attracts more attention from scientists to conduct sustainable oceanographic measurements around these locations (Karlsson and Nordén, 2018; Putri and Pohlmann, 2009; Radjawane and Riandini, 2010; van der Wulp et al., 2016). In contrast, the significantly slower rate of coastal development in these small islands compared with larger islands (Akhir, 2018; World Bank Group, 2018) has attracted less attention from scientists to conduct the similar measurements.

Ambon Island ($\sim$800 km^2; population: $\sim$500,000, source: Indonesian Bureau of Statistics) located in the Coral Triangle region of eastern Indonesia (colored red in Fig. 1a) is the region considered to have the highest risk of marine plastic contamination. As the Maluku provincial capital, Ambon City (red line covering coastal area of Ambon Bay in Fig. 1b) has rapidly developed in recent decades (following the rapid increase of human population in the city; Indonesian Bureau of Statistics, 1980, 2010; Pelasula, 2008), more than development rates in other similarly sized islands, with most development on the island concentrated in this city (Kakisina et al., 2015; Notanubun and Mussadun, 2017). The development in Ambon City has led to a rapid increase in land clearing in the last three decades that has caused increased river runoff during rainfall (Kakisina et al., 2015; Pelasula, 2008; Uneputty and Evans, 1997a). Consequently, Ambon Bay (Fig. 1b), the water body adjacent to Ambon City, has been exposed to marine plastics originating from the city (Manullang, 2019; Suyadi and Manullang, 2020; Uneputty and Evans, 1997a).

Despite the threat, ERA has not been implemented to help evaluate the potential impact of marine plastic accumulation to Ambon Bay with regard to the marine water body of the embayment. While the ERA *probability* of occurrence for the plastic accumulation seems to be clearly defined (i.e. demographic aspects acting as the seeding locations of plastic in Ambon Bay — high population density drives a high *probability* of marine plastic

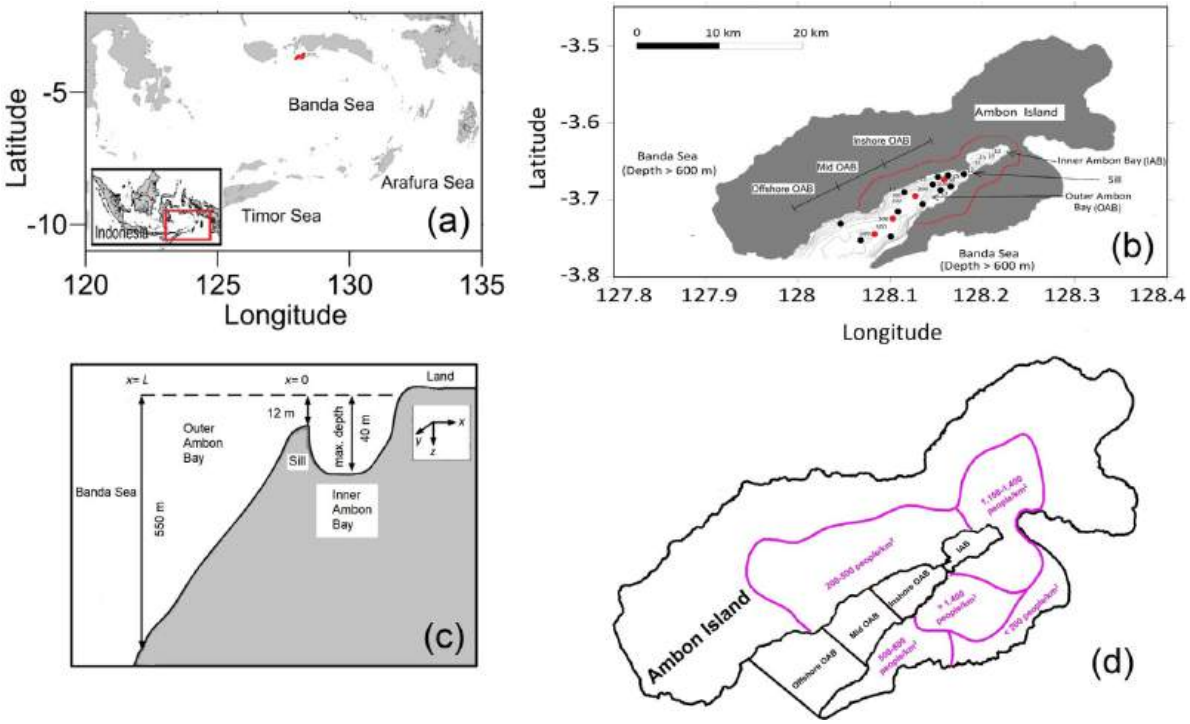

Fig. 1. (a) Banda Sea basin and its surrounding seas; Ambon Island is colored red. (b) The geography of Ambon Bay in which Inner Ambon Bay (IAB) is separated from Outer Ambon Bay by a shallow sill; OAB is considered as three sub-sections (inshore, mid and offshore); bathymetric contours of Ambon Bay are in meters; red line in Ambon Island indicates coastal areas of Ambon City; (•) and (•) represent oceanographic stations from seasonal salinity measurements of the top 50 m and the whole water column, respectively. (c) Schematic depth transect along Ambon Bay consisting of IAB, sill and OAB adjacent to Banda Sea, respectively (not to scale, $L = 22$ km). (d) Human population density at the coastal areas of the sections of Ambon Bay (i.e. IAB, inshore OAB, mid OAB and offshore OAB). . (For interpretation of the references to color in this figure legend, the reader is referred to the web version of this article.)
Source: Indonesian Bureau of Statistics (2010).

accumulation to occur in the coastal waters), the *vulnerability* of Ambon Bay to marine plastics (linked to flushing time) is poorly understood (hence, the level of risk contamination, the end product of ERA, is unknown). Outer Ambon Bay (OAB) is the part of the bay connected to open water (i.e. Banda Sea) and separated from Inner Ambon Bay (IAB) by a shallow sill (Fig. 1b and c). The flushing capacity of Ambon Bay, representing the *vulnerability* of the embayment to marine contaminants including plastics, is only represented by the flushing rate of IAB (∼2 weeks during the peak of rainfall season; Salamena et al., 2021, 2022b) – this is linked to IAB receiving more attention from oceanographic studies due to its fjord basin characteristics that promote pollution build-up (Anderson and Sapulete, 1982; Pello et al., 2014; Salamena et al., 2021, 2022b; Wenno and Anderson, 1984). Insufficient information on the flushing capacity of OAB prevents the implementation of ERA in the entire Ambon Bay.

In this study, we implemented ERA regarding marine plastic accumulation in Ambon Bay by mostly focusing on (i) the demographic distribution along the coasts of Ambon Bay that determine *probability* of occurrence of the plastic accumulation, and (ii) flushing time of Ambon Bay determining *vulnerability* of the embayment to the plastic accumulation. Parts of quantifying *vulnerability* of the entire water body of Ambon Bay, we firstly calculated flushing times of OAB sections (inshore OAB: 0–7.5 km from the sill, mid OAB: 7.5–15 km from the sill; and offshore OAB: 15–22.5 km from the sill; see Fig. 1b and d) and then combined them with the IAB flushing rate obtained from previous studies. The flushing time calculations of OAB employed three techniques (two analytical and one numerical) and only focused on the highest rainfall season (i.e. easterly monsoon, June to August) during which Ambon Bay is highly to be profoundly exposed to marine plastics and experiences a larger onshore–offshore OAB salinity difference (∼1 psu) than in other seasons (∼0.4 psu; Putri et al., 2008) due to high runoff, which is relevant to the rate of flushing. In addition to *vulnerability* linked to flushing, we also regarded the coral ecosystem distribution in Ambon Bay representing ecological values that are exposed to marine plastics — high ecological values (linked to the presence of marine ecosystem) contribute to high *vulnerability* to marine plastic based on previous ERA implementations (Bárcena et al., 2017; Gómez et al., 2014, 2015).

2. Description of oceanography, demography and coastal ecosystem in Ambon Bay

2.1. General oceanography in ambon bay regarding plastic transport and the justifications for using simple flushing models in Ambon Bay

Ambon Bay, a tropical fjord, is a long, narrow bay (Fig. 1b) with a shallow sill (12 m) separating OAB from IAB (Fig. 1b and c). The *vulnerability* to marine contaminants of IAB and OAB during high rainfall season (easterly monsoon) is of great interest to pollution management in Ambon Bay (Anderson and Sapulete, 1982; Pello et al., 2014; Salamena et al., 2022a, 2021; Uneputty and Evans, 1997a). However, to date, only the flushing capacity of IAB has been determined (i.e. ∼2 weeks in the easterly monsoon; Salamena et al., 2021, 2022b) considering the fjordic nature of IAB (Fig. 1b and c).

Tides have the potential to influence the circulation and flushing of OAB. The geomorphology of OAB as a long, narrow embayment results in the predominance of tides in the water circulation

mechanism in the bay, including the surface circulation that controls the dispersal of marine plastics (Hamzah and Wenno, 1987; Wattimena and Salamena, 2022). In contrast, winds (and the resulting surface waves) are unlikely to affect the surface circulation in OAB (and the dispersal of marine plastics) for two main reasons. Firstly, in fjords, the Coriolis effect of winds on water circulation can only be significant when the width of the fjord channel is larger than internal Rossby deformation radius (i.e. controlled by latitudes: the tropics provide very small Coriolis frequency and hence, large Rossby radius; Farmer and Freeland, 1983; Jakacki et al., 2017). OAB, a tropical fjord, has an internal Rossby radius of ~400,000 km, vastly greater than its channel width (4–8 km); hence, wind-driven surface circulation under Coriolis effect is insignificant. Secondly, the mountain range (300–700 m elevation) parallel to the OAB coastlines (Souisa et al., 2016) is likely to weaken winds across the bay and, thus, considerably reduces the effects of winds on the surface circulation (Wattimena and Salamena, 2022).

The geomorphology of OAB (a long, narrow channel) resulting in the tidal predominance and the importance of seasonality (i.e. high rainfall during the easterly monsoon) promote the quantification of OAB flushing using seasonal density balances between inshore OAB (seasonal freshwater inputs) and offshore OAB (oceanic water). There are three primary reasons for this. Firstly, the longitudinal density gradient (i.e. sill-offshore OAB density gradient), typically seasonally-driven, is more important to the net exchange flow than its lateral density gradient (de Silva Samarasinghe and Lennon, 1987; Lavın et al., 1998; Nahas et al., 2005). This physics has been previously studied via longitudinal density balances in other similar systems, including both shallow embayments (<50 m) such as Gulf of St. Vincent, Australia (de Silva Samarasinghe and Lennon, 1987) and Shark Bay, Australia (Nahas et al., 2005); and deep embayments (>50 m) such as Gulf of California, Mexico (Beron-Vera and Ripa, 2000; Jorge et al., 2016; Lavın et al., 1998; Lavín and Marinone, 2003). As a result, the net exchange flow in OAB (and thus flushing time) can be quantified from the density balance between freshwater inputs and onshore–offshore density gradient via an analytical approach for semi-enclosed waters (Andutta et al., 2014; de Silva Samarasinghe and Lennon, 1987). In addition to the longitudinal density balance, there exists a vertically well-mixed condition in most of the OAB water column (near-constant salinity across depths c.a. 50–550 m) with a freshwater surface layer (Tarigan and Wenno, 1991). Together these factors reasonably allow the quantification of the flushing time in OAB (Monismith et al., 2002).

Secondly, the longitudinal density balances and the resulting net exchange process driving flushing in OAB are linked to the tidal flushing mechanism (the predominant circulation component in OAB). In a long oceanic channel system, such as OAB (Fig. 1b), tidal dynamics are represented by periodic water transport of in (flood) and out (ebb) of the system. The resultant transport (i.e. the flood/ebb-averaged flow) behaves as a net/residual flow in the system that can promote flushing of contaminants (including plastics) out of the system (Salamena et al., 2022b). This flood/ebb-averaged flow in oceanic systems with strong density fields (e.g. prevailing onshore–offshore density difference/gradient) is interpreted as equivalent to a steady-state (long-term averaged; e.g. seasonal-mean) density-driven flow due to the longitudinal density balance (de Silva Samarasinghe, 1989; de Silva Samarasinghe and Lennon, 1987; Geyer, 2010). Thus, the application of the longitudinal density balance in OAB, based on seasonal-mean longitudinal density gradient, to investigate OAB flushing predominated by net tidal flow is reasonable.

Thirdly, despite their simplicity, analytical models for flushing time calculation built upon steady-state longitudinal density balance are capable of estimating flushing times comparable with those of the sophisticated numerical models (2D or 3D models). For example, Andutta et al. (2014) provide a comprehensive review on the comparison of analytical models with numerical models in various marine systems; and Salamena et al. (2016) show the agreement of flushing time predicted by an analytical model with that of a 3D numerical ocean circulation model for coastal Great Barrier Reef, Australia.

Table 1
Dimensions of the outer Ambon Bay of eastern Indonesia.

Feature	Values (km)
Width of OAB at the sill, W_{sill}	0.800
Width of OAB at the OAB offshore, $W_{offshore}$	8.385
Depth of the sill, h_{sill}	0.012
Depth of the OAB offshore, $h_{offshore}$	0.550
Distance between the sill and OAB offshore, L	22

2.2. Physical characteristics of outer ambon bay and the related freshwater input in the system to be references for flushing time calculation using longitudinal density balances

The width of OAB increases near linearly with distance from the sill ($x = 0$ at the sill, $x = L$ at the OAB offshore). The surface approximates a trapezium shape of total surface area, $A_{OAB} = 101$ km^2 (Fig. 2; see Appendix for equations). The depth of OAB increases near linearly from the sill to the OAB offshore (Wenno and Anderson, 1984; see also Figs. 1c and 2). The cross-sectional area of OAB can be approximated by parabolic shape (Fig. 2). From this geometry (i.e. depth, width and cross-sectional area), the OAB volume can be approximated as a truncated parabolic pyramid with volume of 23.6 km^3. Details of OAB geometry and volume are illustrated in Appendix and the dimensions of OAB are shown in Table 1.

Freshwater input (m^3/s) to OAB comes from three principal source areas, illustrated in Fig. 2. In general, freshwater input (m^3/s) here employs a steady-state condition (i.e. long-term averaged over seasonal condition — during easterly monsoon) where the difference between precipitation, P, and evaporation, E, results in the net freshwater input ($P - E$; m/s) over a particular area (m^2) (Alestalo, 1983; Dai and Trenberth, 2002). The first freshwater input is ($P - E$) over the OAB surface and surrounds, where P is 22.3 mm/day and E is 4 mm/day for the easterly monsoon (Josey et al., 1998; Yu, 2007). The rate of freshwater input varies with the distance from the sill as $(P - E)\,A1(x)$, where $A1$ is the surface area of OAB from the sill to a distance x offshore. The second freshwater input comes from the river catchment areas along the coasts of OAB. This freshwater input also varies with the distance from the sill, expressed by $(P - E)\,A2(x)$, where $A2(x)$ is a linear fraction (by offshore distance) of the total river catchment area that discharges into OAB, A_{Land_OAB}, determined as 95 km^2 from Siahaya (2016) coupled with the usage of Google Earth's area estimation. The third freshwater input originates from IAB and is related to the total river catchment area in IAB (Siahaya, 2016) plus the surface area of IAB, $A3$ (a total of 56 km^2, Fig. 2), expressed as $(P - E)\,A3$. Combining these three freshwater input components, the advective freshwater input (m^3/s) along the OAB longitudinal section is expressed as:

$$Q(x) = \{A1(x) + A2(x) + A3\}(P - E), \tag{1a}$$

$$where \quad A1(x) = W_{sill} \cdot x + \frac{x^2}{2L}\left(W_{offshore} - W_{sill}\right)$$

$$A2(x) = \left(\frac{x}{L}\right) A_{Land\_OAB}$$

$$A3 = A_{IAB}$$

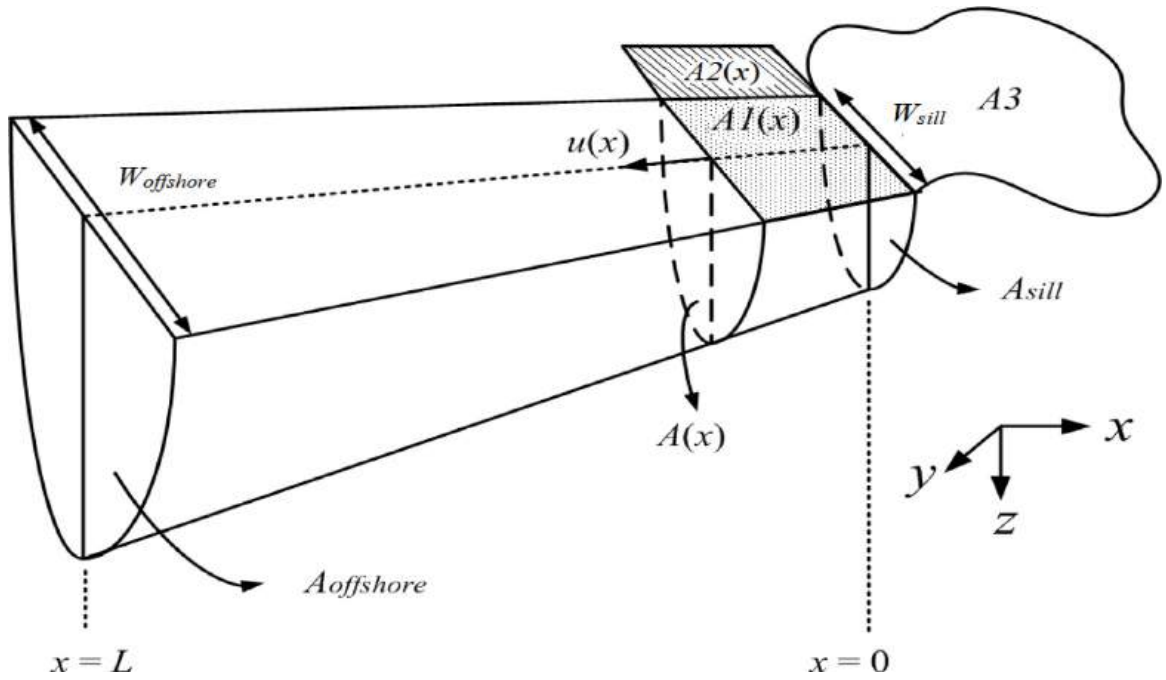

Fig. 2. The schematic diagram of the geometry of OAB used to define variables which are needed to determine $u(x)$; W_{sill}, $W_{offshore}$, $A(x)$, $A1(x)$, $A2(x)$ and $A3$ are explained in the text.

The rate of water exchange (m/s), $u(x)$, averaged over the vertical cross-section of OAB, $A(x)$, can be therefore expressed as:

$$u(x) = \frac{Q(x)}{A(x)} = \frac{\{A1(x) + A2(x) + A3\}(P - E)}{A(x)}, \quad (1b)$$

At the sill ($x = 0$, vertical area A_{sill}), the advective freshwater flow comes entirely from IAB, $u(0) = (P - E)A3/A_{sill}$

2.3. Population, marine plastics and the marine ecosystem distribution in outer Ambon Bay

Human population around Ambon Bay is focused in urban areas. Population density is greater than 1400 people/km^2 along the south coast of the inshore OAB where central business district of Ambon City is located (Indonesian Bureau of Statistics, 2010) and it reduces towards the open ocean with 500–800 people/km^2 occupying the middle and offshore sections of the south coasts of OAB (Indonesian Bureau of Statistics, 2010) (see Fig. 1d). The north coast of OAB does not show the similar abrupt demographic gradient and predominantly has a low population density (200–500 people/km^2) spanning from inshore OAB to some part of offshore OAB (Fig. 1d). The population density around IAB mostly ranges 1100–1400 people/km^2 with small area on the north coast with 200–500 people/km^2 (Fig. 1d).

The quantity of plastics in coastal waters of Ambon Bay is highly correlated with the human population distribution. Higher amounts of plastics are found on the beaches and floating in coastal waters in Ambon Bay such as IAB and inshore OAB where densely-populated areas are located than in the sparsely-populated areas of the middle and offshore sections of OAB (Evans et al., 1995; Uneputty and Evans, 1997a).

Coastal marine ecosystem diversity follows an opposite gradient to human population density. Higher density and more diverse coral reefs are found in the middle and offshore sections of OAB compared with the inshore OAB and IAB (McManus and Wenno, 1981; Syahailatua et al., 2012). Similarly, the diversity and abundance of reef fish associated with coral reefs (e.g. *Chaetodontidae*) increase towards the offshore OAB (Bawole, 1998).

3. Data and methods

3.1. Flushing time calculation in outer Ambon Bay

3.1.1. Archival data used for flushing time calculation

Salinity data used in this study were acquired between 2008 and 2012 from only the months June to August, reflecting the easterly monsoon (Mudjiono, 2009; Putri et al., 2008; Salamena, 2010, 2011, 2012). The locations of these salinity measurements are shown as (•) and (•) in Fig. 1b, which were measured within the top 50 m and the whole water column, respectively. For the top 50 m measurements, the CTD used was an Alec Compact CTD (Alec Electronics Co., Ltd., Kobe, Japan) with the accuracy of salinity and temperature of ±0.01 psu and ±0.01°C, respectively while the whole water column measurements were conducted using Sea-Bird SBE 19plus V2 from Research Vessel Baruna Jaya VII (accuracy, salinity: ±0.00007 psu; temperature: ±0.0001 °C).

Since salinity changes slowly below the top 50 m in the OAB longitudinal section (Tarigan and Wenno, 1991), the surface salinity data (top 50 m, stations (•) in Fig. 1b) were combined with the deep data (stations (•), Fig. 1b) to produce total depth-averaged salinity data along the OAB longitudinal section (Fig. 3). The effect of freshwater significantly reduces towards open ocean, as shown by the increased average and decreased range of salinity values with increased distance from the sill (Fig. 3) – the inshore OAB (0–7.5 km from the sill) has larger salinity range compared with that in the mid (7.5–15 km from the sill) and the offshore OAB (15–22.5 km from the sill).

3.1.2. Methods to calculate flushing time in outer Ambon Bay

3.1.2.1. Land-Ocean Interaction Zone (LOICZ) model. Land–Ocean Interaction Coastal Zone (LOICZ) model is an analytical model for estimating the coastal-oceanic exchange flow and the flushing time of coastal waters and estuaries (Andutta et al., 2014; Swaney et al., 2011). Practically, the flushing time estimated using the LOICZ model is the ratio between the volume of coastal waters, V, and the net flow consisting of the total freshwater inputs in

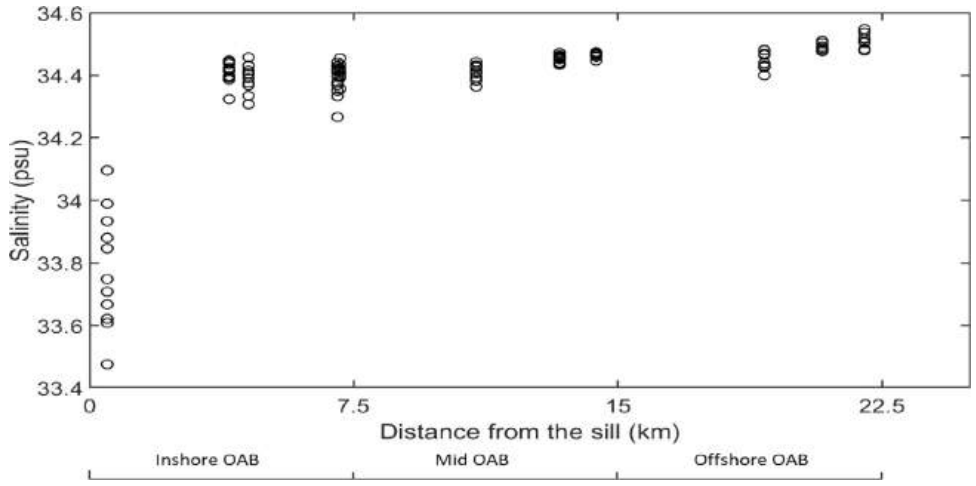

Fig. 3. Total depth-averaged salinity (psu) obtained from measurements in the OAB longitudinal-section during the easterly monsoon (June to August) between 2008 and 2012; the station configuration of these oceanographic measurements is shown by Fig. 1b.

a system and the coastal-oceanic exchange flow due to coastal-oceanic density gradient (Andutta et al., 2014). The OAB flushing time for the LOICZ model is given by

$$\tau = \frac{V}{Q_R + 0.5Q_R\left(S_o + \bar{S}\right) / \left(S_o - \bar{S}\right)} \tag{2}$$

where $\bar{S}$ is the average measured salinity, S_o is the Banda Sea salinity and Q_R is the total freshwater volume rate (unit: m^3/s), quantified as:

$$Q_R = (P - E)\left(A_{OAB} + A_{Land\_OAB} + A3\right) \tag{3}$$

The LOICZ model can also be used to identify whether horizontal advection or horizontal diffusion is the predominant mechanism controlling the flushing process in a marine system (Andutta et al., 2014). This is achieved by decomposing the flushing time formula (Eq. (2)) into advective and diffusive components, $\tau_{advection}$ and $\tau_{diffusion}$, respectively (Andutta et al., 2014) as follows:

$$\frac{1}{\tau} = \frac{1}{\tau_{advection}} + \frac{1}{\tau_{diffusion}}; \tag{4}$$

where $\tau_{advection} = \frac{V}{Q_R}$; and $\tau_{diffusion} = \frac{V}{0.5Q_R(S_o+\bar{S})/(S_o-\bar{S})}$

Advective predominance is identified when $\left(\frac{1}{\tau_{diffusion}}\right)$ is considerably smaller than $\left(\frac{1}{\tau_{advection}}\right)$ (Andutta et al., 2014).

3.1.2.2. Salt-exchange model. Modeling of salt-exchange processes provides a second analytical estimate of the e-folding flushing time for coastal waters, given by (Salamena et al., 2016; Wang et al., 2007):

$$\tau = \frac{h\,(x)\,(S_o - S\,(x))}{(S_o \cdot q)}, \tag{5}$$

where S_o is the offshore salinity, and $S(x)$ is salinity at a particular distance of x from the sill with a depth of $h\,(x) = h_{sill} + \left(\frac{h_{offshore} - h_{sill}}{L}\right) x$ (see Appendix). The equivalent precipitation rate, q (unit: m/s), is the effective net vertical freshwater input if the freshwater input from all sources, Q_R, (see Eq. (3)) is distributed evenly across the surface of OAB; i.e.,

$$q = \frac{(P - E)\left(A_{OAB} + A_{Land\_OAB} + A3\right)}{A_{OAB}} \tag{6}$$

Combining Eqs. (5) and (6) allows for calculation of the flushing time of OAB to the open ocean, but can also be used to analyze the exchange of the sub-sections of OAB to the open ocean (see Wang et al. (2007) for the application to cross-shelf sections of the Great Barrier Reef, Australia). Here, we employed long-term average salinity data along the OAB longitudinal section (Fig. 3) with constant offshore salinity, S_o, to estimate the flushing time of water within the OAB longitudinal section.

3.1.2.3. 1D advection–diffusion model. The 1D advection–diffusion numerical model (hereinafter referred as the 1D model) used here is similar to that of Wang et al. (2007) that utilized salinity as a conservative passive tracer to study horizontal mixing in the coastal hypersaline system in Great Barrier Reef (GBR), Australia. By constraining their analysis to the dry season of northern Australia, Wang et al. (2007) could define freshwater inputs from rain or rivers as negligible. Here, we advance the application of the 1D model for the OAB system where freshwater inputs are significant. The heart of the 1D model applied in the OAB system during the easterly monsoon is that the advective flux of salt out of OAB due to the net outward water flow from river discharge and direct rainfall is balanced by an inward diffusive flux of salt driven by the higher salinity water offshore.

Using the geometry and variables from Figs. 2 and 4, the salt exchange for OAB can be expressed as

$$\frac{\partial S\,(x)}{\partial t} = \frac{\partial S\,(x)}{\partial x}\left(k\,(x)\left\{\frac{m}{h\,(x)} + \beta\right\} - u\,(x)\right) - S\,(x)\left(\frac{m}{h\,(x)}u\,(x) + \frac{\partial u\,(x)}{\partial x}\right) + k\,(x)\,\frac{\partial^2 S\,(x)}{\partial x^2} \tag{7}$$

where

- $m = \left(\frac{h_{offshore} - h_{sill}}{L}\right)$
- $k(x)$ is the longitudinal diffusion coefficient which is assumed to vary exponentially as $k(x) = k_o \exp\,[-\,\beta\,(L - x)]$, where k_o is the diffusion coefficient at the offshore OAB and β is the decay coefficient of horizontal diffusion
- $u(x)$ (see Eq. (1b)) is the advective flow speed of water out of the bay due to rivers and direct rainwater input; and
- $\frac{\partial u(x)}{\partial x}$ in Eq. (7) indicates the spatial variation of $u(x)$ along OAB, expressed by:

$$\frac{\partial u}{\partial x} = \frac{(P - E)\left(\lambda A_{sill} + 2\,(\gamma \cdot A_{sill} - \psi \cdot A3)\,x - \psi\lambda x^2\right)}{(A\,(x))^2}$$

$$\lambda = \left(W_{sill} + \frac{A_{Land\_OAB}}{L}\right);\ \gamma = \left(\frac{W_{offshore} - W_{sill}}{2L}\right);$$

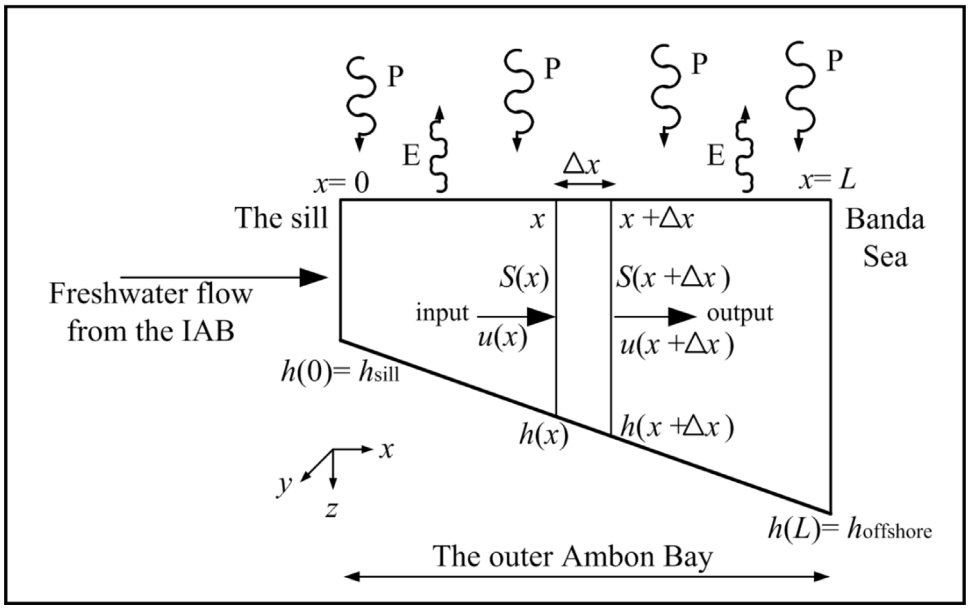

Fig. 4. Longitudinal section of OAB describing salinity and freshwater flux and geometry. The water depth increases linearly from the sill; and the freshwater flow at the sill is from IAB.

$$\psi = \left(\frac{A_{offshore} - A_{sill}}{L^2}\right) \tag{8}$$

Parameters β and k_o were determined by numerically solving Eq. (7) for the steady-state condition ($\partial S / \partial t = 0$) using the observed salinity. A range of different values for each of β and k_o was anticipated given the envelope of observed salinity (cf. Wang et al., 2007). The numerical scheme for the first and second spatial derivatives of $S(x, t)$ utilized the centered difference approximation following Wang et al. (2007); i.e., $\frac{\partial S}{\partial x} = \frac{S(x+\Delta x)-S(x-\Delta x)}{2\Delta x}$ and $\frac{\partial^2 S}{\partial x^2} = \frac{S(x+\Delta x)-2S(x)+S(x-\Delta x)}{\Delta x^2}$, respectively.

The boundary conditions of salinity are as follows. The boundary condition for $S(x, t)$ at the OAB-Banda Sea boundary ($x = L$) was the assumed constant salinity ($S = 34.51$ psu) representing Banda Sea water (Waworuntu et al., 2000). In contrast, the boundary condition of salinity at the sill ($x = 0$) was set to balance the landward diffusive flux of salt and the seaward freshwater flux at the sill; i.e. $u(x)\ S(x) = k(x)\frac{\partial S(x)}{\partial x}$. Due to the absence of an extra numerical grid landward after the sill, the forward difference scheme was numerically applied for the first spatial derivative of salinity i.e. $\frac{\partial S}{\partial x} = \frac{S(x+\Delta x)-S(x)}{\Delta x}$ instead of the centered difference scheme. The boundary condition of salinity at the sill numerically becomes $u(x)\ S(x) = k(x)\frac{S(x+\Delta x)-S(x)}{\Delta x}$, and the salinity at the sill, $S(x = 0)$, can be computed as:

$$S(x=0) = \frac{S(\Delta x)}{\left(1 + \frac{u(0)}{k(0)}\Delta x\right)}, \tag{9}$$

where $S(\Delta x)$ is estimated using Eq. (7). The boundary conditions of $u(x)$ and $k(x)$ at the sill are $u(0) = (P - E)A3/A_{sill}$ and $k(0) = k_o \exp(-\beta L)$, respectively.

Once the values of k_o and β are determined by fitting the model output to observed salinities, the flushing time of OAB was estimated using the steps of Wang et al. (2007). For the entire OAB (i.e. between $x = 0$ and $x = L$), the steps of the flushing time calculation are as follows. (1) For the 1D model, the concentration of a conservative tracer, C replaced the concentration of salt, S in Eq. (7). (2) Initially, C was uniform for the model domain between $x = 0$ and $x = L$; the integration of C over the whole OAB longitudinal section is the initial mass of solute, M_o. (3) Eq. (7) was solved numerically to calculate the change of the concentration spatially and temporarily with the boundary condition of concentration at the sill ($x = 0$) following Eq. (9) i.e. $C(x = 0) = C(\Delta x) / \left(1 + \frac{u(0)}{k(0)}\Delta x\right)$ and the boundary condition of zero concentration was applied at the OAB-Banda Sea boundary ($x = L$). (4) The flushing time was defined as the timescale required for the mass of solute, M_o within the OAB to decay to 37% M_o (Andutta et al., 2013; Deleersnijder et al., 2006; Wang et al., 2007).

The calculation of flushing time within the sections of OAB followed that for the entire OAB. The adjustment only prevails for the initial condition, that is, C will be imposed in a particular section of interest in OAB such as between the sill ($x = 0$) and a certain distance from the sill and $C = 0$ will be set to the remaining numerical grids.

3.2. Environmental risk assessment regarding marine plastics in Ambon Bay

3.2.1. Theoretical framework: insights from Gómez et al. (2015)

3.2.1.1. General introduction. Environmental risk assessment (ERA) is considered to be a well-established, generic quantitative instrument to evaluate the potential impacts of threats to environment and thus, is of great general interest to environmental management and the related policy-making at multiple levels (Gómez et al., 2014, 2015; Hope, 2006; Mazarrasa et al., 2019; Suedel et al., 2008). In general, ERA provides information on (i) environmental threats (i.e. their nature and magnitude) by quantifying the *probability* of occurrence of the threats (P_i); (ii) the *vulnerability* of the environment to the threats (V_i); and (iii) the *consequences* of the threats (C_i) (Gómez et al., 2014, 2015). The combination of these components forms environmental risk (R_i) expressed as (Gómez et al., 2015; Mazarrasa et al., 2019):

$$R_i = P_i \times V_i \times C_i \tag{10}$$

The application of ERA is variable depending on types of environmental risk investigated (Gómez et al., 2014, 2015; Hope, 2006; Mazarrasa et al., 2019; Suedel et al., 2008). For this study where the environmental risk (i.e. marine plastic accumulation in water body) is related to flushing capacity, it adopts ERA based on Gómez et al. (2015; linking flushing capacity to environmental risk on water quality in marine system)

Probability, P_i, relates to the likelihood of exposure to the threat. It may be defined by an observed frequency of events (Gómez et al., 2015) or known characteristics of the threat (such as the availability of plastics). *Vulnerability*, V_i, is defined as the characteristic of the environment that has the potential to be harmed (Birkmann, 2007; Gómez et al., 2014, 2015). *Vulnerability* is a function of *susceptibility* of the environment to threats, SU_i. It is also dependent upon the *state of conservation*, indicating the value of the environment at risk, that is contributed by: (i) *naturalness* (NA_i), the absence of physical anthropogenic modifications, and (ii) *ecological value* (EV_i), the capacity of the environment in harboring ecosystem (Gómez et al., 2014, 2015). Combining these three parameters, *vulnerability*, V_i, is expressed as (Gómez et al., 2015):

$$V_i = 1/3 \left\{ \underbrace{2 \times SU_i}_{Susceptibility} + \underbrace{(1/3) \times (NA_i + 2 \times EV_i)}_{State\ \ of\ \ conservation} \right\} \quad (11)$$

Consequences, C_i, from the threats may be environmental and/or societal. Impacts to the environment (*discharge impact*) are assessed through evaluation of *hazardousness*, HZ_i (the nature of the threats), and *extent*, EX_i (affected area due to threats) (Gómez et al., 2015). The social/public response to the threats (*social impact*) is informed by *adopted measures*, AM_i (the responses of public in dealing with the threats), and *social repercussion*, SR_i (public awareness of the threats) (Gómez et al., 2015). Combining these parameters, the *consequences* term, C_i, is expressed as (Gómez et al., 2015):

$$C_i = 1/3 \left\{ \underbrace{(HZ_i + EX_i)}_{Discharge\ \ impact} + \underbrace{(1/2) \times (AM_i + SR_i)}_{Social\ \ impact} \right\}. \quad (12)$$

3.2.1.2. Practical implementations. For the grading of risk, R_i (Eq. (10)), in implementing ERA based on Gómez et al. (2015), three categories were employed: *high-risk contamination source* ($R_i > 30$), *moderate-risk contamination source* ($10 < R_i \leq 30$), and *low-risk contamination source* ($R_i \leq 10$). In addition, the practical implementations of ERA based on Gómez et al. (2015) regarding *probability*, *vulnerability*, and *consequences* parameters and the related assessment criteria are presented in Table 2. The assessment criteria were valued using a four-point scale; i.e. very high (i.e. V; score: 4), high (i.e. H; score: 3), moderate (i.e. M; score: 2), and low (i.e. L; score: 1).

For *probability*, P_i, Gómez et al. (2015) used the frequency of discharge events; here, the human population density is employed (Table 2). Gómez et al. (2015) represented *susceptibility* by flushing time characteristics around European ports (on a scale from less than 1 day indicating low *susceptibility* to more than 30 days representing very high *susceptibility*, Table 2); here, this approach is adopted with modifications to the category thresholds relevant to Ambon Bay (Table 2). The definition of *naturalness* (a state of conservation parameter) by the absence/presence of physical anthropogenic modifications (e.g. the presence of bridges, dikes, wharf; Bárcena et al., 2017; Gómez et al., 2014) is similarly adopted (see Table 2). *Ecological value* (another state of conservation parameter) was represented by Gómez et al. (2015) based on the presence/absence of ecological singular elements (ESE; Table 2); e.g. protected areas, habitats for flora/fauna; here, this term is represented using coral reefs as an indicator for ESE, with additional resolution within the range of values based on different habitat types (Table 2).

For *consequences*, C_i, the definitions of Gómez et al. (2015) were adopted. For *discharge impact*, *hazardousness* was defined by the types of substances discharged into the environment and the *extent* affected as a proportion of the total area (Table 2). *Social impact* considered *adopted measures* based operating procedures (OP) to address/tackle environmental threats (ranging from the absence to specific/maintained procedures) (Table 2); and *social repercussion* categorized by the level of social alarm resulting from environmental threats (ranging from no social alarm to high media coverage and/or invoking citizen actions) (Table 2).

3.2.2. Justifying modifications of ERA for Ambon Bay and the subsequent implementation

While most of the assessment criteria of ERA from Gómez et al. (2015) in Table 2 were relevant to risk assessment of marine plastic accumulation in Ambon Bay, there were three major modifications made to suit the context of risk assessment in Ambon Bay. Firstly, for *probability* (Table 2), *the probability of occurrence* of marine plastics was employed, linked to the demographic distribution in the coastal areas of the bay (Fig. 1d) behaving as the seeding locations of plastics (Fok and Cheung, 2015; Li et al., 2016; Mahoney, 2017). Here, the assessment criteria for *the probability of occurrence* were graded as very high for very high population density (score: 4), high (high population density, score: 3), moderate (moderate population density, score: 2), and low (low population density, score: 1). In addition, very high *probability* (score: 4) of the occurrence of marine plastics was also applied to the IAB based on the high degree of isolation of the fjord basin coupled with surrounding high population (Suyadi and Manullang, 2020) (Fig. 1d). This very high *probability* status with similar geomorphologic-demographic settings was previously reported in an Artic fjord (Adventfjorden) with low coastal population density (due to small settlements in the remote location) that can drive significant marine plastic accumulation (Herzke et al., 2021).

The second modification for ERA in this study was the grading of *susceptibility* to marine plastic accumulation in Ambon Bay linked to the magnitude of flushing time. Flushing time is highly variable from one water body to another depending on the local and regional physical oceanographic processes prevailing in a marine system, with flushing timescales ranging from daily (Andutta et al., 2014; Bárcena et al., 2017) to weekly (Andutta et al., 2013; Choukroun et al., 2010; Salamena et al., 2016, 2021, 2022b; Wang et al., 2007), monthly (Andutta et al., 2013; Chen et al., 2019; Choukroun et al., 2010; Collins et al., 1997; Das et al., 2000; de Silva Samarasinghe and Lennon, 1987; Kämpf et al., 2010) and yearly-to-decadal (Ffield and Gordon, 1992; Guo et al., 2016; Stigebrandt and Aure, 1989; Xu and Zheng, 1991). As such, the grading of *susceptibility* to plastic accumulation in a marine system needs to be locally relevant, considering the maximum local flushing time representing very high *susceptibility* (the maximum score that determines the grading system) (e.g. Bárcena et al., 2017; the use of the maximum value of local flushing time). For Ambon Bay, the grading of *susceptibility* to plastic accumulation should be based on the flushing capacity of IAB (i.e. ~2 weeks; Salamena et al., 2021, 2022b) as the maximum flushing timescale in the Ambon Bay system (considering its most isolation to the open ocean). As a result, *susceptibility* categories were defined as (Table 2): very high (score: 4; $\tau \geq 2$ weeks), high (score: 3; 1.5 weeks $< \tau < 2$ weeks), moderate (score: 2; 1 week $< \tau < 2$ weeks), and low (score: 1; $\tau \leq 1$ week).

The third modification was the assessment criteria of *ecological singular elements* (ESE; see Table 2). We elaborated the general criteria of ESE of Gómez et al. (2015; Very high, V = 4 indicating the presence of ESE; Low, L = 1 indicating the absence of ESE; see Table 2) to accommodate the coral ecosystem diversity along the coasts of Ambon Bay (i.e. reduced diversity towards IAB, see Section 2.3). The grading of ESE used in this study (Table 2) was: high diversity of corals (score: 4; typically, light-reliant corals in offshore and mid OAB), low diversity corals (predominantly,

Table 2
Parameters and assessment criteria of Gómez et al. (2015) with some modifications for Ambon Bay.

Parameter			Assessment criteria	
			From Gómez et al. (2015; their Table 3)	This study
Probability	*Occurrence*	*Occurrence*	*Frequency of occurrence* (F) of a discharge from a contaminant source	*Probability of occurrence* of marine plastic based on coastal population density (PD), coupled with fjordic attributes
			V = 4 F ≤ 7 days H = 3 7 d < F ≤ 30 d M = 2 30 d < F ≤ 365 d L = 1 F > 365 d	V = 4 Very high PD/fjordic basin H = 3 High PD M = 2 Moderate PD L = 1 Low PD
Vulnerability	*Susceptibility*	*Susceptibility*	*Flushing time* (τ) of the water domain where a contaminant source is located	
			V = 4 τ > 30 d H = 3 7 d < τ ≤ 30 d M = 2 1 d < τ ≤ 7 d L = 1 τ ≤ 1 d	V = 4 $\tau \geq$ 2 weeks H = 3 1.5 w ≤ τ < 2 w M = 2 1 w < τ < 1.5 w L = 1 τ ≤ 1 w
	State of conservation	*Naturalness*	*Alteration by hydromorphological pressures* (HP) where a contaminant source is located	
			V = 4 Not altered by HP L = 1 Altered by HP	V = 4 Not altered by HP
		Ecological value	*Ecological singular elements* (ESE) where a contaminant source is located	
			V = 4 Presence of ESE L = 1 Absence of ESE	H = 4 High diversity, light-reliant corals M = 3 Low diversity, turbid-tolerant corals L = 1 Absence of corals
Consequences	*Discharge impact*	*Hazardousness*	*Discharge substances or handled materials* by a contaminant source	
			V = 4 Priority hazardous substances H = 3 Priority substances M = 2 Dangerous materials L = 1 Potential dangerous materials or others	V = 4 Plastics are priority hazardous substances
		Extent	*Affected area* (%) of each water domain by contaminant source	
			V = 4 % ≥25 H = 3 5 < % ≤ 25 M = 2 1 < % ≤ 5 L = 1 % < 1	L = 1 % < 1
	Social impact	*Adopted measures*	*Efficiency of operating procedure* (OP) related to a contaminant source	
			L = 4 OP not available M = 3 Generic OP available H = 2 Specific OP available V = 1 Specific/maintained OP/personnel trained	M = 3 Generic OP available
		Social repercussion	*Level of social alarm* of a contaminant source	
			V = 4 Events in TV/citizen acts H = 3 Events in press M = 2 Citizen complaints L = 1 No social alarm	V = 4 Events in TV/citizen acts

turbid-tolerant corals around inshore OAB to the sill; score: 3), and near absence of corals (typically in IAB; score: 1) (McManus and Wenno, 1981; Pelasula et al., 2022; Syahailatua et al., 2012).

For the ERA regarding marine plastic accumulation in Ambon Bay, parameters that varied along the longitudinal section of Ambon Bay were *probability* of occurrence of marine plastics derived from the population density (Fig. 1d), *susceptibility* to plastic accumulation linked to the distribution of flushing time (i.e. τ of IAB from (Salamena et al., 2021, 2022a,b) combined with τ of OAB obtained from this study; Section 3.1), and *ecological singular elements* represented by coral ecosystem diversity along Ambon Bay.

In contrast, several other assessment criteria were constant for all sections of Ambon Bay (OAB and IAB) following certain grades based on the context of Ambon Bay (Table 2). *Naturalness* of Ambon Bay related to flushing was set as very high for the entire Ambon Bay (V; score: 4; Table 2). This was despite evidence of increased land clearings in Ambon Bay (in 1996 and 2020; Fig. 5a and b) and small changes in the geomorphology of Ambon Bay, including coastal contours (surface areas of the Ambon Bay sections remained essentially unchanged). For *hazardousness*, plastics were categorized as hazardous substances due to their harmful effects to the environment (hence, V; score: 4, Table 2) (Li et al., 2016; Lithner et al., 2011; Rochman et al., 2013). This assessment criterion was applied to the entire Ambon Bay due to the predominance of plastic debris in the marine litter composition in the embayment (Manullang et al., 2021). For *extent*, this study applied "low affected area" (i.e. < 1% of the total area of surface water body; score: 1; Table 2) due to the small-scale patchiness of plastic accumulation sites visible in the water body of Ambon Bay (see Fig. 5c–e). The *adopted measures* to tackle marine plastic accumulation in Ambon Bay was rated to be at a moderate level (i.e. only generic operating procedure available; score: 3; Table 2) due to sporadic spatial and temporal aspects of beach and marine (using a net from small boats) plastic clean-ups that have been conducted voluntarily (BeritaBeta.com, 2020; Herdiansyah et al., 2021; Uneputty et al., 1998; Wattimena et al., 2023). The *social impacts* criterion was rated to be very high (score: 4; Table 2) due to a wide media coverage of marine plastic accumulation in Ambon Bay and the campaign on beach clean-ups in Ambon Bay by local communities (BeritaBeta.com, 2020; Herdiansyah et al., 2021; Uneputty et al., 1998; Wattimena et al., 2023).

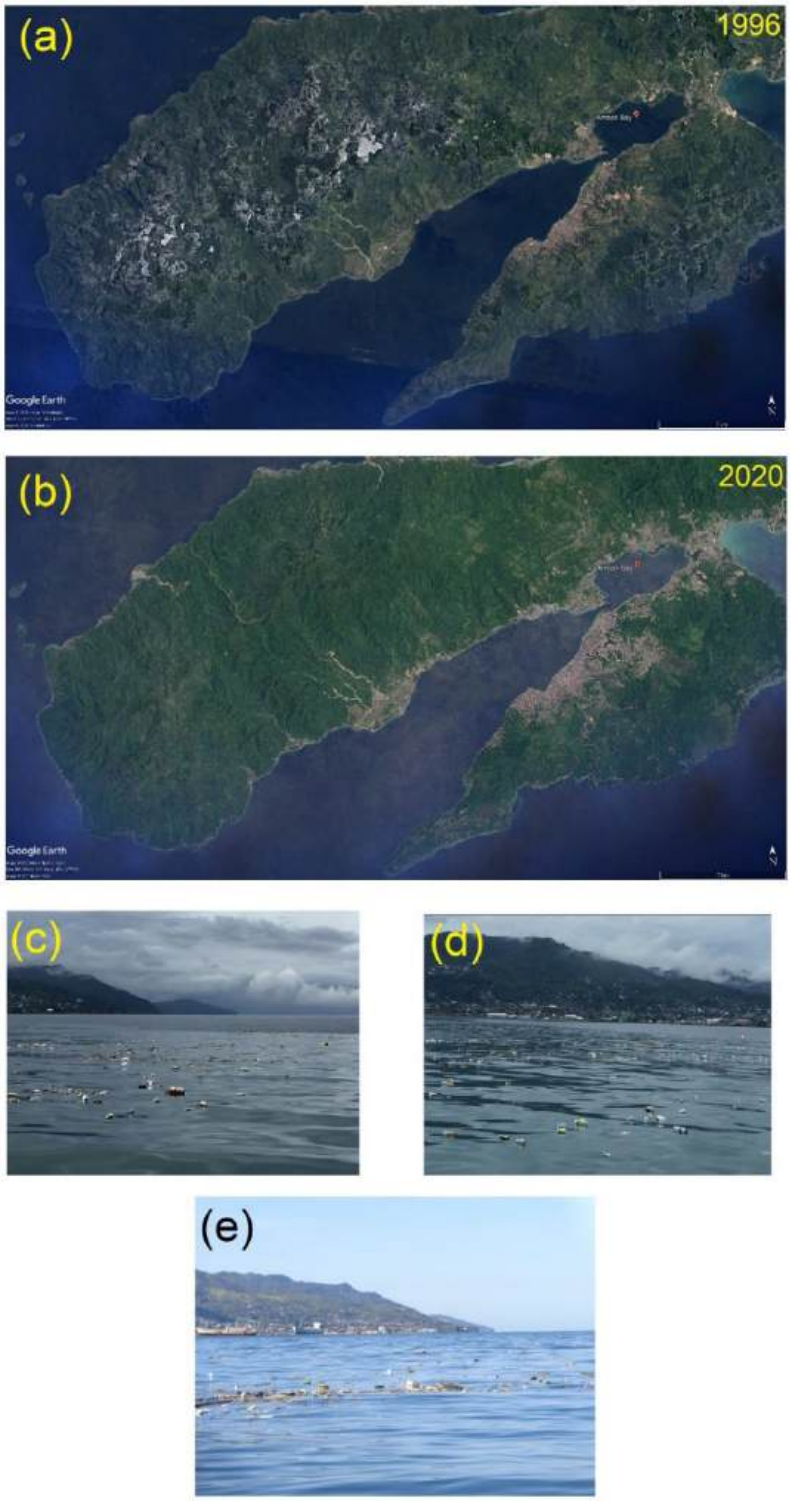

Fig. 5. The historical satellite images of Ambon Bay in (a) 1996 and (b) 2020. Patchiness of plastic accumulation sites in the water body of Ambon Bay in July 2019 (c and d) and March 2018 (e); source: personal documentations (i.e. (c) and (d) – Gerry Salamena) and online news (i.e. (e); link: link: https://menaraglobal.com/2018/03/23/teluk-ambon-darurat-sampah/).

4. Results

4.1. Flushing time calculations of outer Ambon Bay

4.1.1. The entire basin and related sub-sections

Flushing time of the entire OAB during the easterly monsoon was found to be 1–1.5 weeks. Using the LOICZ model with Q_R, V, S_o and $\overline{S}$ values of 53.37 $\pm$ 7 m^3/s, 23.6 $\pm$ 1.1 km^3, 34.51 $\pm$ 0.06 psu and 34.45 $\pm$ 0.06 psu, respectively, the flushing time of the entire OAB was found to be 9 $\pm$ 2 days. The uncertainty of Q_R ($\pm$7 m^3/s) was contributed to precipitation, evaporation and the Google Earth's horizontal length error for estimating river catchment areas in OAB and IAB and the IAB surface area ($\pm$172 m; Potere, 2008), which also contributed to the

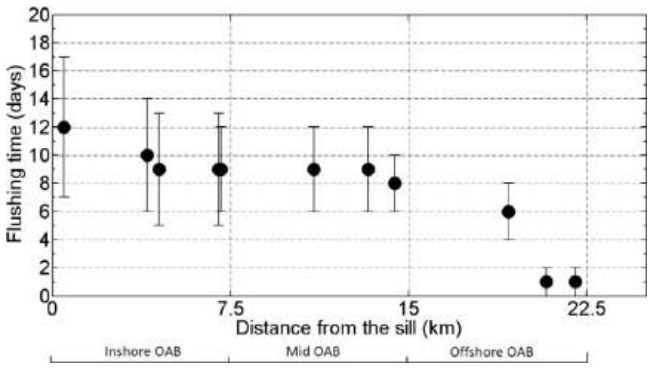

Fig. 6. The flushing times of water at various distances from the sill in the OAB longitudinal section calculated using the salt-exchange model (Eq. (5)).

uncertainty in V ($\pm$1.1 km^3). The uncertainty in the salinity values ($\pm$0.06 psu) was obtained from Fig. 3. The flushing time of the entire OAB using the salt-exchange model was calculated by averaging flushing times of all data points between the sill and the offshore OAB in Fig. 6 as 8 $\pm$ 3 days; the uncertainties in the salt-exchange model were similarly contributed as for the LOICZ model. Additionally, the flushing time of the entire OAB predicted by the 1D model was 5 $\pm$ 3 days. This was based on the definition that flushing time is the timescale for the total mass of material to decay from a total initial mass, M_o, to be 37% M_o (Fig. 7a). The flushing time calculated by the 1D model (Fig. 7a) employed the optimum offshore horizontal diffusion coefficients, k_o, (i.e. 90 m^2/s, 160 m^2/s and 317 m^2/s) and β (i.e. 5 $\times$ 10^{-6} m^{-1}) which enabled the salinity predicted by the 1D model to graphically fit for the observed salinity as shown in Fig. 7b (see Figs. 8 and 12 of Wang et al., 2007 analogiously to Fig. 7a and b in this current study).

The flushing times of sub-sections of OAB were determined using the salt-exchange and 1D models. The flushing times of the inshore OAB predicted by the salt-exchange model and the 1D model were approximately 10 $\pm$ 1 days (see Fig. 6) and 11 $\pm$ 6 days (Fig. 8a), respectively. The flushing time of the mid OAB was 9 $\pm$ 1 days by the salt-exchange model (Fig. 6) and 7 $\pm$ 4 days by the 1D model (Fig. 8b). The flushing time of water located at the offshore OAB was predicted to be 3 $\pm$ 2 days from the salt-exchange model (Fig. 6) and 2 $\pm$ 1 days from the 1D model (Fig. 8c). Additionally, these models can be used to determine the flushing time of the combined inshore and mid OAB sub-sections (i.e. water located between the sill and 15 km from the sill). The flushing time predicted by the salt-exchange model for this OAB sub-section was ca. 9 days (see Fig. 6) while from the 1D model was found to be 9 $\pm$ 5 days (Fig. 8d).

4.1.2. Predominant renewal mechanisms

The flushing of OAB waters is predominated by horizontal turbulent diffusion, driven by the density gradient between OAB and Banda Sea. From the LOICZ model (using Eq. (4)), the advective timescale, $\tau_{advection}$ (5175 $\pm$ 440 days) is orders of magnitude larger than the diffusive timescale, $\tau_{diffusion}$ (9 $\pm$ 1 days). As a result, $\left(\frac{1}{\tau_{advection}}\right)$ is considerably smaller than $\left(\frac{1}{\tau_{diffusion}}\right)$ in Eq. (4), therefore, indicating diffusive predominance. The agreement between the 1D model and the analytical models (i.e. salt-exchange and LOICZ models) in predicting flushing times of OAB and its sub-sections, despite their methodological differences, further supports the predominance of diffusive process in controlling the net water renewal in OAB.

4.2. Environmental risk assessment regarding marine plastic accumulation in Ambon Bay

The *probability* for the occurrence of marine plastics in Ambon Bay was linked to coastal density population as the seeding

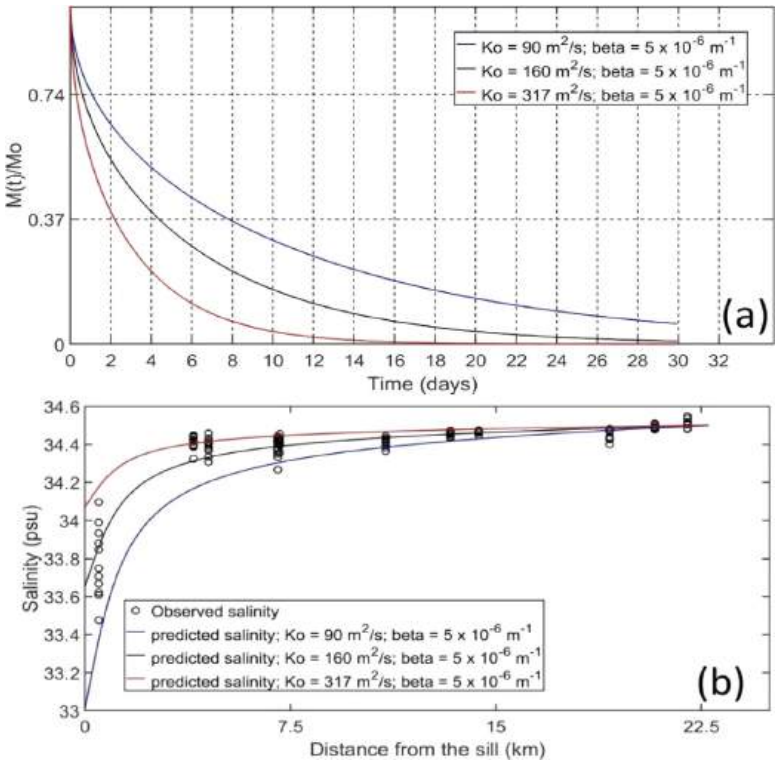

Fig. 7. (a) Relative mass of concentration ($M(t)/M_o$) remaining within OAB after an initial concentration, M_o, imposed within the OAB longitudinal section; the zero concentration was applied at the OAB-Banda Sea boundary ($x = L$). (b) Predicted longitudinal-section salinity distributions (psu) in the OAB after 90 day run (i.e. June–August period) using the best k_o and β in order to fit the observed salinity.

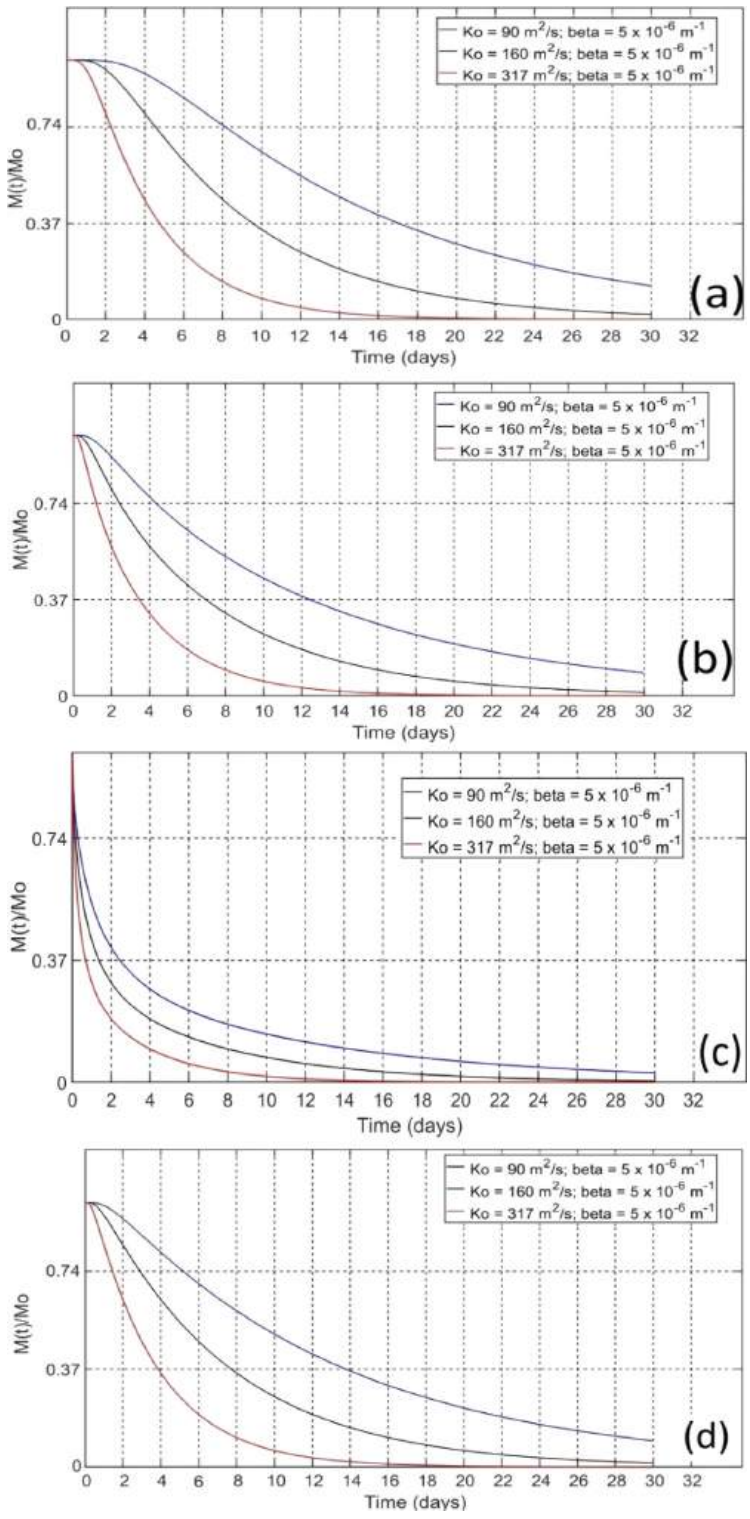

Fig. 8. Relative mass of concentration ($M(t)/M_o$) remaining within (a) inshore OAB, (b) mid OAB, (c) offshore OAB and (d) the combined inshore and mid OAB. This is similar to Fig. 7a.

locations of plastics and fjord characteristics (Fig. 9a). The fjordic nature of IAB (with shallow sill entrance) coupled with high coastal population density (i.e. 1100–1400 people/km^2 at the south; 200–500 people/km^2 at the north; Fig. 9a) led IAB to have very high *probability* for the occurrence of marine plastics (score: 4). The inshore OAB was also assigned very high *probability* due to its very high population density (i.e. >1400 people/km^2 at the south coast; 200–500 people/km^2 at the north coast; Fig. 9a). Mid-OAB has significantly lower coastal population density than inshore OAB and IAB (500–800 people/km^2 at the south coast coupled with 200–500 people/km^2 at the north coast; Fig. 9a) and was assigned a moderate *probability* (score: 2). Offshore OAB presented a low *probability* (score: 1) due to its sparsely populated coasts (500–800 people/km^2 at the south coast; Fig. 9a).

The *susceptibility* of the water body of Ambon Bay to marine plastic accumulation was linked to flushing capacity during the

easterly monsoon (Eq. (11)). IAB was assigned a very high *susceptibility* (score: 4) due to the longest flushing time ($\tau = \sim 2$ weeks; Fig. 9b). Inshore OAB displayed a high *susceptibility* (score: 3; $\tau = 1.5$ weeks $< \tau < 2$ weeks) while mid-OAB presented a moderate *susceptibility* (score: 2; $\tau = 1$ week $< \tau < 1.5$ weeks; Fig. 9b). Offshore OAB exhibited a low *susceptibility* (score: 1; $\tau \leq 1$ week; Fig. 9b).

The *vulnerability* of Ambon Bay to marine plastic accumulation (Fig. 9c) resulted from combining of the *susceptibility* (Fig. 9b) and *state of conservation* components (using Eq. (11), values in Table 2). IAB and inshore OAB were determined to have high *vulnerability* (score: 3), whilst mid and offshore OAB sections displayed a moderate *vulnerability* (score: 2). The *consequences* score (Eq. (12)) was relatively high (score: 2.8) over all sections of Ambon Bay due to the constant assessment criteria (Table 2).

Combining the scores of *probability*, *vulnerability* and *consequences*, the level of risk of marine plastic accumulation (Eq. (10)) in IAB ($R_i = 38$) and inshore OAB ($R_i = 35$) was high (Fig. 10); mid-OAB exhibited a moderate risk ($R_i = 15$); and offshore OAB displayed a low-risk plastic accumulation ($R_i = 5$; Fig. 10).

5. Discussion

5.1. Flushing time of Outer Ambon Bay

The determined flushing time for OAB for the easterly monsoon is less than the range of values from previous studies in embayments with similar aspect ratio to OAB. Spatial aspects (i.e. length and volume) of OAB seem to be key factors to produce shorter flushing time than other studied semi-enclosed waters. Flushing times of other long, narrow bays were reported as more than three months; e.g., 130 days and 300 days for St. Vincent Gulf (140 km long) and Spencer Gulf (320 km long), respectively; 100–200 days for Gulf of California (1500 km) (Collins et al., 1997; de Silva Samarasinghe and Lennon, 1987; Kämpf et al., 2010). This scale of duration was also reported for semi-enclosed waters with large surface area (hence, large volume) despite shallow depths (<30 m) such as Sydney Harbour estuary of Australia ($\tau = 225$ days; maximum depth: 28 m; surface area: 52 km^2) (Das et al., 2000; Tanner et al., 2017) and Bohai Sea of China ($\tau = \sim 1000$ days using a passive tracer analysis; average depth: 18 m; surface area: 77,000 km^2) (Guo et al., 2016; Xu and Zheng, 1991). In contrast, OAB has a short length (22 km) and hence, small volume (~24 km^3) despite having deep seaward entrance (up to 550 m, Fig. 1b and c). As such, OAB is more likely to be rapidly flushed by the open ocean (Abdelrhman, 2005; Collins et al., 1997), consistent with the determined shorter flushing time (1–1.5. weeks).

The geomorphology of OAB (i.e. a roughly straight bay with wide seaward entrance; Fig. 1b) seems to be a key factor to produce a shorter flushing time than similar size embayments with complicated geomorphologies. For instance, Coffin Bay estuary (length: 25 km; surface area: 125 km^2) with similar aspect ratio to OAB has comparable spatial aspects to OAB (length: 22 km; surface area: 101 km^2) and yet, has a considerably longer flushing time (~50 days; obtained from the mean flushing time of all sections of the estuary; Kämpf and Ellis, 2015; Fig. 9) than OAB (1–1.5 weeks). This longer flushing time of the entire Coffin Bay estuary is linked to narrow seaward entrance coupled with interconnected bays within the estuarine basin that separate the inner section of this estuary from rapid flushing at the offshore section (comparable in magnitude with OAB), causing an order of magnitude difference in the flushing time between these two sections (i.e. ~90 days for the inner section *cf.* 10 days for the offshore section) (Kämpf and Ellis, 2015). The simpler geomorphology of OAB (see Fig. 1b) results in only a slight difference in the flushing time between the inshore OAB (1–1.5 weeks) and the offshore OAB (1–6 days).

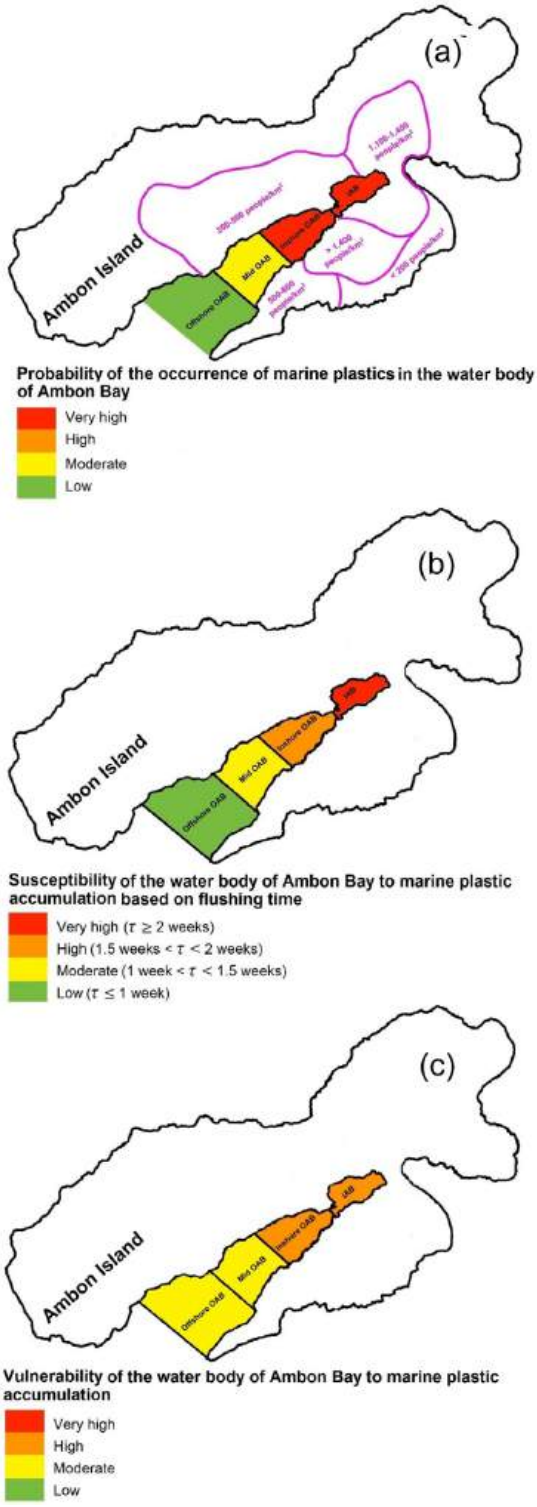

Fig. 9. (a) Probability of the occurrence of marine plastics in the water body of Ambon Bay. (b) Susceptibility of the water body of Ambon Bay to marine plastic accumulation based on flushing time. (c) Vulnerability of the water body of Ambon Bay to marine plastic accumulation.

The longitudinal variation of flushing times of the sub-sections of OAB is in agreement with previous related studies. The flushing time in OAB increases with increasing distance from the open ocean (see. Figs. 6 and 8). This is consistent with longer flushing

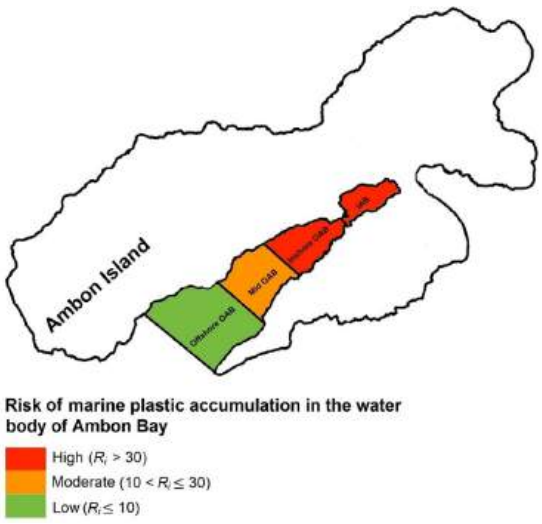

Fig. 10. Risk of marine plastic accumulation in the sections of Ambon Bay.

time found in the inshore section than in the offshore section of St. Vincent Gulf, Spencer Gulf and Coffin Bay estuary of South Australia (de Silva Samarasinghe and Lennon, 1987; Kämpf and Ellis, 2015; Kämpf et al., 2010).

The mathematical expressions of the salt-exchange model (Eq. (5)) and the LOICZ model, particularly diffusive flushing time (i.e. $\tau_{diffusion}$, Eq. (4)), indicate that a larger inshore–offshore salinity difference produces longer flushing time. The OAB-Banda Sea salinity difference during the easterly monsoon (∼1 psu, see Fig. 3) (Putri et al., 2008; Tarigan and Wenno, 1991) is larger than that of the westerly monsoon (December to February) and transitional seasons (March to May and September to November) (i.e. ∼0.4 psu) (Putri et al., 2008). As such, the flushing times of OAB and its sub-sections during the easterly monsoon are expected to be longer than in other seasons and therefore are useful to describe the vulnerability to marine plastics.

In addition to the flushing time calculation in OAB, this study enables adequate information on flushing capacity in Ambon Bay. Prior to this study, the information on the flushing rate of Ambon Bay was only represented by the flushing capacity of IAB (Salamena et al., 2021, 2022b). The quantification of flushing time of OAB in this study now provides a complete insight into the flushing capacity of Ambon Bay (see Fig. 9b) that is of interest to coastal and marine ecosystem management in the embayment.

One immediate impact from adequate information on flushing capacity in Ambon Bay is to describe the distribution of coastal marine ecosystem diversity along the longitudinal section of Ambon Bay. Turbidity-tolerant corals are predominantly found in the inshore OAB and IAB, which are characterized by high total suspended solids concentrations (McManus and Wenno, 1981; Pelasula, 2008; Syahailatua et al., 2012). The presence of turbid water in the inshore OAB and IAB is likely to be related to slow flushing process in this location (Fig. 9b) which can contribute to the accumulation of suspended solids (Elliott and Whitfield, 2011; McLusky and Elliott, 2004). In contrast, a higher diversity of living corals is abundantly found in the coasts of the mid and offshore OAB, including those with greater reliance upon high light conditions for photosynthesis (Fabricius, 2005; McManus and Wenno, 1981; Stanley, 2006). In these sub-sections the higher water clarity (Syahailatua et al., 2012) is likely linked to the rapid flushing process (Fig. 9b).

5.2. Risk assessment in Ambon Bay regarding marine plastic accumulation

The degree of risk of Ambon Bay to marine plastic accumulation is controlled by the demographic and oceanographic characteristics of the embayment. IAB presented a high risk to marine plastic accumulation (Fig. 10). This status was partly linked to very high *probability* of occurrence of marine plastics driven by the high population density along most of the IAB coast (Fig. 9a) that acts as the source of plastics (Fok and Cheung, 2015; Li et al., 2016; Mahoney, 2017). The other factor resulting in high risk for IAB was high *vulnerability* (Fig. 9c) to plastic accumulation associated with slow flushing. IAB has the maximum flushing time in the Ambon Bay system (Fig. 9b) due to its farthest inshore location and oceanographic isolation by the shallow sill. High risk of marine plastic accumulation was also apparent for the inshore OAB with similar demographic-oceanographic characteristics (Fig. 10). Ambon City provides the highest population density of the bay, producing a very high *probability* parameter (Fig. 9a). Combining this with the high *vulnerability* due to slow flushing (distant from the open ocean; de Silva Samarasinghe and Lennon, 1987; Kämpf and Ellis, 2015; Kämpf et al., 2010), led to the assessed high risk. Assessments of moderate risk in mid OAB and low risk in offshore OAB (see Fig. 10) were due to moderate *vulnerability* to plastic accumulation (Fig. 9c; resulting from shorter flushing times, Fig. 9b), coupled with moderate and low *probability* of occurrence, respectively, due to low population density surrounding these OAB sections (Fig. 9a). Note that high risk of plastic accumulation in IAB and inshore OAB described here (representing the easterly monsoon) was qualitatively confirmed by the observation (Uneputty and Evans, 1997a; during the easterly monsoon) reporting a generally increasing amount of marine plastics in the surface layer towards IAB.

The demographic-oceanographic combination in Ambon Bay promoting high-risk plastic accumulation in the embayment is consistent with other studies, here and elsewhere. Plastic accumulation in the surface layer of IAB and inshore OAB was observed during the easterly monsoon, with generally increasing amounts of marine plastics towards IAB (Uneputty and Evans, 1997a), similarly linked to slow flushing and high human population density. The Bohai Sea of China has a long flushing time (τ > 1 year; very high *vulnerability*) and is surrounded by very highly urbanized and industrialized zones in China (very high *probability*; Guo et al., 2016; Li et al., 2015; Xu and Zheng, 1991; Zhu et al., 2020), resulting in a high amount of marine plastic accumulation (Li et al., 2018; Zhang et al., 2017). The oceanographic and demographic factors driving marine plastic accumulation in inshore OAB and IAB are also similar to those prevailing in the semi-enclosed basin of Maowei Sea (China). Maowei Sea has long flushing time (τ > 3 months; at least high *vulnerability*) due to its isolation from the open ocean (Chen et al., 2019) and is fed by large river systems whose catchments are located in densely populated areas in China mainland (very high *probability*) (Zhang et al., 2020; Zhu et al., 2019). These factors are consistent with the high amount of marine plastics observed (Zhu et al., 2021, 2019).

5.3. Some notes on the ERA application in Ambon Bay

Despite the ERA application in this study providing valuable information for marine plastic management in Ambon Bay (Figs. 9 and 10), it is also worthwhile commenting on how the ERA implementation can be advanced in future studies. The main improvement to assessing the *vulnerability* to plastic accumulation in coastal areas of Ambon Bay would be to further elaborate on the flushing time (*susceptibility*) as plastics are flushed out from their source locations (Critchell et al., 2019). This requires

higher-dimensional numerical models that apply virtual tracers representing marine plastics (e.g. 2D or 3D numerical models; Critchell et al., 2019; Soto-Navarro et al., 2020). Unlike the simple models (analytical and 1D numerical) used in this study that provide generic information of water transport processes in Ambon Bay via flushing timescales, more-sophisticated numerical models can monitor the movement of virtual tracers and, thus, determine locations in the coastal areas of Ambon Bay where marine plastics transit before being flushed out to the open ocean (Critchell et al., 2015; Critchell and Lambrechts, 2016). There is probability that some marine plastics can be beached during the flushing process (Critchell et al., 2015). As such, assessing the spatial distribution of plastic exposure (area where plastics transit in coastal areas) in Ambon Bay could identify coastal areas/beaches most likely to experience buildup of plastics within high-risk sections (IAB, inshore OAB; Fig. 10).

The application of ERA in Ambon Bay, especially *vulnerability* related to flushing capacity, can also be expanded to other marine contaminants in the embayment (e.g. dissolved pollutants dispersed following water movements). Flushing time, a transport timescale determining how long water parcels stay within a marine basin before being flushed out, is of general interest to marine pollution management since the water transport timescale can represent the degree of pollution build-up in the system (Andutta et al., 2014, 2013; Wang et al., 2007). Beyond plastic accumulation, Ambon Bay particularly IAB is vulnerable to contaminants such as (i) turbid water due to sediment discharge from upper land of the embayment during peak rainfall season (Pelasula, 2008) and (ii) the accumulation of organic materials from aquaculture sites (feeds and feces) in IAB that can drive eutrophication (Murtiono et al., 2015; Tett et al., 2011). The ERA implementation on these contaminants could provide important insights into the degree of risk contamination in IAB that can be used for the pollution mitigation and management in the water basin.

5.4. Lessons from Ambon Bay to other coastal waters in Indonesian' Coral Triangle region regarding the potential applications of ERA

The use of flushing time in assessing the *vulnerability* of Ambon Bay to marine plastic accumulation is likely to be applicable for most reef systems in Indonesia's Coral Triangle. Fringing reefs, like those in Ambon Bay particularly in OAB, are the most common coral reef formation in Indonesia's Coral Triangle, especially near the island coastlines of eastern Indonesia (Burke et al., 2012). Their level of exposure to the open ocean together with water exchange processes characterizes their *vulnerability* to the accumulation of marine pollution, including plastics (Umar et al., 1998; Wang et al., 2007). Some fringing reefs located in semi-enclosed bays of this Coral Triangle region, such as Cendrawasih Bay of Western New Guinea (length: ~300 km) and Weda Bay of Halmahera Island (length: 70 km), are appropriate candidates for a *vulnerability* assessment (Djamhur et al., 2014; Mangubhai et al., 2012). Fringing reefs in more open systems, where alongshore transport exists besides cross-shore transport (though with a small density gradient), might also be suitable for this vulnerability assessment. Examples of locations with this characteristic include: Tuhaha Bay and Saparua Bay in Saparua Island; Piru Bay of Ceram Island, Maluku Archipelago (Sahetapy et al., 2018; Sapulete, 1996); Misool Island (~2000 km^2) of Raja Ampat archipelago, the location of the world's highest coral biodiversity (Mangubhai et al., 2012); and Kaimana and other locations along the continental shelf of Western New Guinea (Mangubhai et al., 2012). Similar investigations of flushing time have previously been undertaken in open systems, including the central Great Barrier Reef shelf of Australia (Hancock, 2006; Mao and Ridd, 2015; Wang et al., 2007).

In addition to flushing time estimations in this study, this pioneering study on ERA regarding plastic accumulation in the coastal water body in eastern Indonesia paves ways for similar studies, including for other types of pollutants, in locations across the Indonesian Coral Triangle region. Information on flushing capacity (a key parameter for quantifying *susceptibility*) in islands of eastern Indonesia is limited due to scarce oceanographic observations (typically season specific) driven by the remoteness of the islands (Ardania et al., 2019; Basit and Putri, 2013; Nurhayati, 2006; Putri et al., 2008; Sapulete, 1996). This contrasts to the information of marine biodiversity (a key parameter for the *state of conservation*) and marine degradation linked to pollution (a key parameter for *consequences*) in the region (Ceccarelli et al., 2022; Edinger et al., 1998, 2000; Hutubessy and Mosse, 2023; Ismail et al., 2021; Limmon and Manuputty, 2021; Limmon et al., 2023; Mangubhai et al., 2012; Sahetapy et al., 2021, 2018). The flushing models used in this study (i.e. salt-exchange model, LOICZ model and 1D advection–diffusion model; see Section 3.1.2) require relatively easy-to-measure parameters, such as seasonal density variations and the dimensions of marine system (depth, volume). As such, they provide a practical tool to estimate flushing time in the coastal waters of remote islands in eastern Indonesia. Together with the abundant information of marine biodiversity and degradation in the region, this would allow the implementation of ERA in other locations in the Coral Triangle region regarding pollutant accumulation.

6. Concluding remarks

6.1. Flushing time of outer Ambon Bay

This study calculated flushing time (τ) of OAB to complement the IAB flushing timescale previously obtained (i.e. 2 weeks; Salamena et al., 2021, 2022b) in order to provide a complete insight into the flushing capacity in Ambon Bay. The flushing time of the entire OAB was found to be 1–1.5 weeks. Inshore OAB was found to be flushed within 1.5–2 weeks while τ of mid OAB was found to be 1–1.5 weeks. The flushing time of offshore OAB was $\leq$ 1 week.

6.2. Environmental risk assessment

This study presents the first environmental risk assessment of marine plastic accumulation in Ambon Bay during the peak rainfall season (easterly monsoon; when plastic discharge into the bay is greatest) by considering (i) the *probability* of occurrence of marine plastics, linked to coastal population density; (ii) the *vulnerability* of Ambon Bay, linked to flushing capacity (i.e. τ) in the longitudinal section of the embayment and the longitudinal distribution of marine ecosystem diversity; and (iii) the *consequences* of plastic accumulation. The risk of marine plastic accumulation in Ambon Bay was found to be high in IAB and inshore OAB, with moderate and low risk in mid OAB and offshore OAB, respectively.

6.3. Future studies regarding flushing in Ambon Bay

The flushing time calculation in this study was focused on onshore–offshore density gradient to drive the flushing process and determine vulnerability to marine plastics. However, there are other factors that could be addressed in potential future studies. Despite the effective implementation of the 1D model for the longitudinal OAB section, the model does not consider secondary circulations occurring in water close to coasts of OAB. Estuarine circulation due to freshwater outflow at the river mouths of the OAB coasts could influence the small-scale dispersal of marine

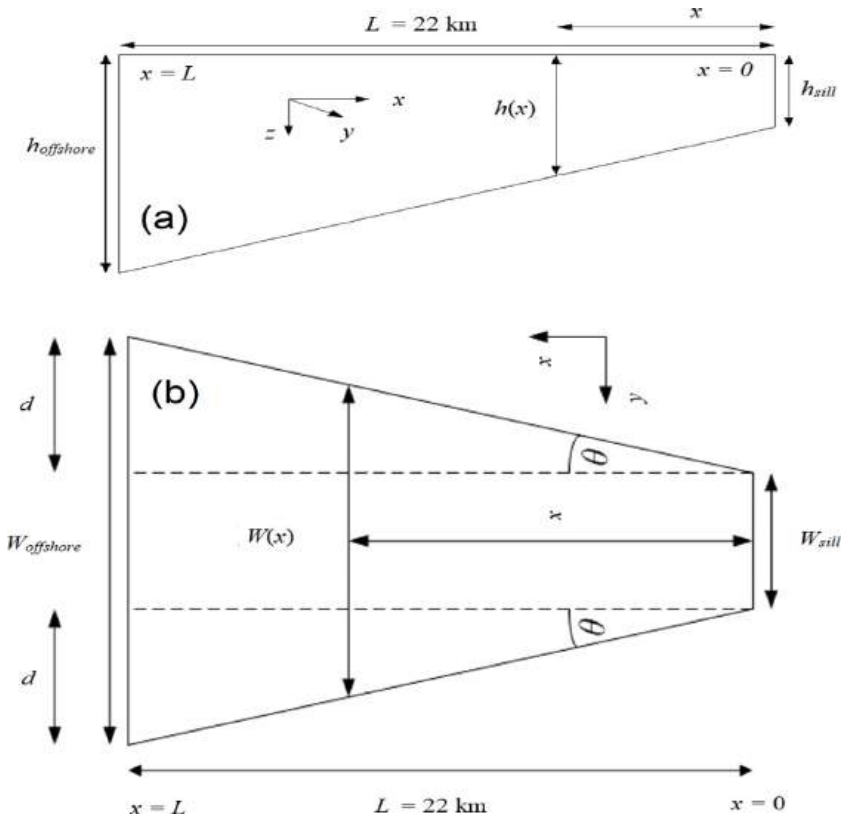

Fig. A.1. Schematic diagram of Outer Ambon Bay from (a) longitudinal and (b) plane views.

plastics. In addition, the bathymetric slope of the inshore OAB might drive tidal pumping around the sill (Salamena et al., 2021) that can affect surface circulation (and influence the dispersal of marine plastics). As such, it is recommended that these secondary circulations be investigated using a 3D baroclinic model.

Nonetheless, the consistency of flushing times derived from the three methods presented supports the outcomes and their application to inform the management of marine pollution in Ambon Bay.

CRediT authorship contribution statement

Gerry Giliant Salamena conceptualized the original research idea of this paper, conducted data curation, visualization, scientific analysis and wrote the original draft and revised it based on constructive feedback from co-authors. **Scott F. Heron and Peter V. Ridd** were fundamental in improving the theoretical framework of the analytical formulas of the used models in this paper and providing narrative on plastic managements linked to flushing process. They were also reviewing and editing the original draft. **James C. Whinney** was involved later in improving data analysis, reviewing, and editing the original draft.

Declaration of competing interest

The authors declare that they have no known competing financial interests or personal relationships that could have appeared to influence the work reported in this paper.

Data availability

The authors do not have permission to share data.

Acknowledgments

The authors gratefully acknowledge the oceanographic datasets (i.e. the top 50 m water column) used in this manuscript that were obtained from Oceanographic Monitoring Program in Ambon Bay spanning 2007–2012 by Centre for Deep-Sea Research of Indonesian Institute of Sciences – LIPI (now, National Research and Innovation Agency – BRIN) based in Ambon City with special thanks to (i) Dr. Augy Syahailatua (the director of the institution at that time) who mostly facilitated the program and (ii) the CTD operators of the institution. The authors also would like to thank the same institution for the access of CTD data from its Research Vessel Baruna Jaya VII that measured the density of the whole water column in the longitudinal OAB section. The authors would like to thank two anonymous reviewers for their constructive comments to substantially improve the manuscript.

Appendix

A.1. Approximated geometry of outer Ambon Bay

The geometry of outer Ambon Bay (OAB) can be approximated as linearly increases of depth and width along the bay. The depth of OAB is expressed as

$$h(x) = h_{sill} + \left(\frac{h_{offshore} - h_{sill}}{L}\right) x, \tag{A.1}$$

where x is distance from the sill, h_{sill} and $h_{offshore}$ are respectively the depths at the sill ($x = 0$) and at the OAB offshore ($x = L$) and L (22 km) is the distance between the sill and OAB offshore (see Fig. A.1a).

The surface area of OAB approximates a trapezium (Fig. A.1b) compared with its physical shape in Fig. 1b. The width of OAB

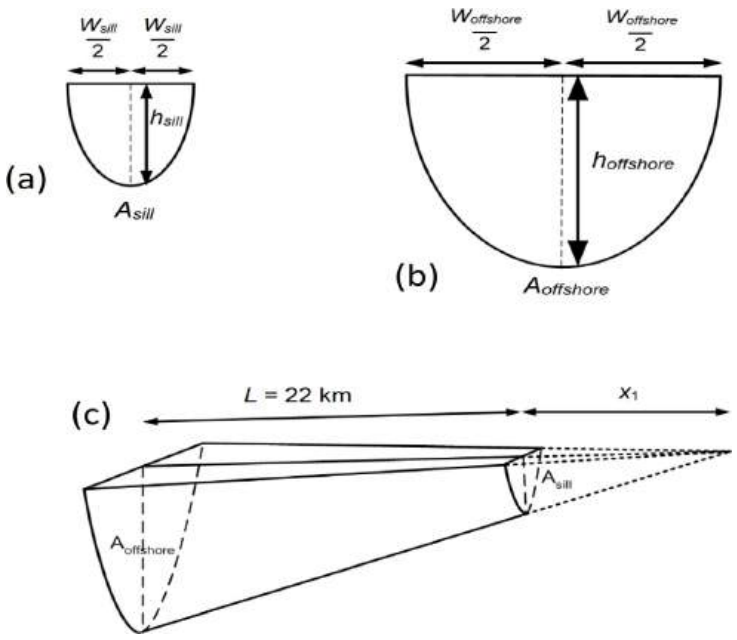

Fig. A.2. (a) and (b) are cross-sectional areas at the sill and at the OAB-Banda Sea boundary. (c) The application of truncated pyramid features on the geometry of the OAB.

increasing with distance from the sill is expressed as

$$W(x) = W_{sill} + \left(\frac{W_{offshore} - W_{sill}}{L}\right) x \tag{A.2}$$

where W_{sill} and $W_{offshore}$ are respectively the widths of OAB at the sill and at the OAB offshore. The surface area of OAB as a function of distance from the sill is thus expressed as

$$A1(x) = 0.5\,(W_{sill} + W(x))\,x = 0.5\left(2W_{sill} + \left(\frac{W_{offshore} - W_{sill}}{L}\right) x\right) x, \tag{A.3}$$

The surface area of entire OAB, A_{OAB}, when $x = L$ and $W(L) = W_{offshore}$ is 101 km^2 using the values in Table 1.

The vertical cross-section of OAB is represented as a parabola (Fig. A.2a and b). The linear increase in depth, width, and surface area of OAB section with distance from the sill consequently causes the parabolic cross-sectional areas of OAB, $A(x)$, to vary with the square of distance from the sill shown in Eq. (A.4).

$$A(x) = A_{sill} + \left(\frac{A_{offshore} - A_{sill}}{L^2}\right) x^2 \tag{A.4a}$$

$$A_{sill} = \frac{4}{3}\left(\frac{W_{sill}}{2}\right) h_{sill} \tag{A.4b}$$

$$A_{offshore} = \frac{4}{3}\left(\frac{W_{offshore}}{2}\right) h_{offshore} \tag{A.4c}$$

The parabolic cross-sectional areas at the sill, A_{sill}, (Eq. (A.4b)) and at the OAB offshore, $A_{offshore}$, (Eq. (A.4c)) are respectively 0.0064 km^2 and 3.07 km^2.

A.2. Calculation of volume of outer Ambon Bay

We calculated the volume of the OAB, V_{OAB}, following the approximated geometry described in Appendix A.1. This resulted in a truncated cone shape with parabolic base area (Fig. A.2c). The OAB dimensions in Fig. A.2a and b (i.e. width and depth at the sill and the offshore) are found in Table 1.

V_{OAB} is computed as the volume difference between pyramid with base area of $A_{offshore}$ and pyramid with base area of A_{sill} with the application of an imaginary length of x_1 which was applied to enable the application of the volume formula of pyramid (see Fig. A.2c). The value of x_1 was firstly determined before computing V_{OAB} by utilizing the relationship between base areas and heights of pyramid as shown in Eq. (A.5) and was found to be approximately 1.05 km. Thus, V_{OAB} was mathematically calculated by using Eq. (A.6) and was found to be ca. 23.6 km^3.

$$\left\{\frac{x_1}{(L + x_1)}\right\}^2 = \frac{A_{sill}}{A_{offshore}}, \tag{A.5}$$

$$V_{OAB} = \underbrace{\left((1/3) \cdot A_{offshore} \cdot (L + x_1)\right)}_{\text{volume of pyramid with } A_{offshore}} - \underbrace{\left((1/3) \cdot A_{sill} \cdot x_1\right)}_{\text{volume of pyramid with } A_{sill}} \tag{A.6}$$

References

Abdelrhman, M.A., 2005. Simplified modeling of flushing and residence times in 42 embayments in New England, USA, with special attention to Greenwich Bay, Rhode Island. Estuar. Coast. Shelf Sci. 62, 339–351.

Akhir, K., 2018. A Critical Analysis of Technological Interventions Towards the National Action Plan for Marine Litter Management 2018-2025: Recommendations for Addressing Marine Plastic Litter in the 'New Balis' of Indonesia Sustainably. World Maritime University, Malmo, Sweden, p. 86.

Alestalo, M., 1983. The atmospheric water vapour budget over Europe. Var. Glob. Water Budget 67–79.

Anderson, J.J., Sapulete, D., 1982. Deep water renewal in inner Ambon Bay, Ambon, Indonesia. In: Gomez, E.D., Birkeland, C.E., Buddemeier, R.W., Johannes, R.E., Marsh, Jr., J.A., Tsuda, R.T. (Eds.), The 4th International Coral Reef Symposium. Marine Science Center of University of Philippines, Manila, Phillippines, pp. 370–374.

Andutta, F.P., Ridd, P.V., Deleersnijder, E., Prandle, D., 2014. Contaminant exchange rates in estuaries – New formulae accounting for advection and dispersion. Prog. Oceanogr. 120, 139–153.

Andutta, F.P., Ridd, P.V., Wolanski, E., 2013. The age and the flushing time of the Great Barrier Reef waters. Cont. Shelf Res. 53, 11–19.

Ardania, D., Kamal, M.M., Wardiatno, Y., 2019. Keterkaitan parameter fisika-kimia perairan dengan kemunculan hiu paus (rhincodon typus) di perairan teluk cendrawasih papua. In: Simposium Nasional Hiu Pari Indonesia. pp. 279–284.

Bakir, A., Rowland, S.J., Thompson, R.C., 2014. Transport of persistent organic pollutants by microplastics in estuarine conditions. Estuar. Coast. Shelf Sci. 140, 14–21.

Bárcena, J.F., Gómez, A.G., García, A., Álvarez, C., Juanes, J.A., 2017. Quantifying and mapping the vulnerability of estuaries to point-source pollution using a multi-metric assessment: The Estuarine Vulnerability Index (EVI). Ecol. Indic. 76, 159–169.

Basit, A., Putri, M., 2013. Water mass characteristics of Weda Bay, Halmahera Island, North Maluku. J. Teknol. Kelaut. Trop. 5, 365–376.
Bawole, R., 1998. Spatial Distribution of Chaetodontidae Fish and Its Roles As the Indicator of Coral Reef Condition in Ambon Bay (in Indonesian Language). Bogor Institute of Agriculture, p. 88.
BeritaBeta.com, 2020. Miris, Netizen Keluhkan Warga Terus Buang Sampah Di Teluk Ambon. BeritaBeta.com.
Beron-Vera, F.J., Ripa, P., 2000. Three-dimensional aspects of the seasonal heat balance in the Gulf of California. J. Geophys. Res.: Oceans 105, 11441–11457.
Birkmann, J., 2007. Risk and vulnerability indicators at different scales: Applicability, usefulness and policy implications. Environ. Hazards 7, 20–31.
Boerger, C.M., Lattin, G.L., Moore, S.L., Moore, C.J., 2010. Plastic ingestion by planktivorous fishes in the North Pacific Central Gyre. Mar. Pollut. Bull. 60, 2275–2278.
Broderick, A.C., Duncan, E.M., Nelms, S.E., Godley, B.J., Galloway, T.S., Godfrey, M.H., Hamann, M., Lindeque, P.K., 2015. Plastic and marine turtles: a review and call for research. ICES J. Mar. Sci. 73, 165–181.
Bugoni, L., Krause, L.g., Virgınia Petry, M., 2001. Marine debris and human impacts on sea turtles in Southern Brazil. Mar. Pollut. Bull. 42, 1330–1334.
Burke, L., Reytar, K., Spalding, M., Perry, A., 2012. Reefs at risk revisited in the Coral Triangle.
Ceccarelli, D.M., Lestari, A.P., White, A.T., 2022. Emerging marine protected areas of eastern Indonesia: Coral reef trends and priorities for management. Mar. Policy 141, 105091.
Chen, Z., Qiao, F., Wang, G., Xia, C., 2019. Sensitivity of the half-life time of water exchange in coastal waters. Sci. China Earth Sci. 62, 643–656.
Choukroun, S., Ridd, P.V., Brinkman, R., McKinna, L.I., 2010. On the surface circulation in the western Coral Sea and residence times in the Great Barrier Reef. J. Geophys. Res.: Oceans 115.
Choy, C.A., Drazen, J.C., 2013. Plastic for dinner? Observations of frequent debris ingestion by pelagic predatory fishes from the central North Pacific. Mar. Ecol. Prog. Ser. 485, 155–163.
Collins, C.A., Garfield, N., Mascarenhas, Jr., A.S., Spearman, M.G., Rago, T.A., 1997. Ocean currents across the entrance to the Gulf of California. J. Geophys. Res.: Oceans 102, 20927–20936.
Connors, E.J., 2017. Distribution and biological implications of plastic pollution on the fringing reef of Mo'orea, French Polynesia. PeerJ 5, e3733.
Critchell, K., Grech, A., Schlaefer, J., Andutta, F.P., Lambrechts, J., Wolanski, E., Hamann, M., 2015. Modelling the fate of marine debris along a complex shoreline: Lessons from the Great Barrier Reef. Estuar. Coast. Shelf Sci. 167, 414–426.
Critchell, K., Hamann, M., Wildermann, N., Grech, A., 2019. Predicting the exposure of coastal species to plastic pollution in a complex island archipelago. Environ. Pollut. 252, 982–991.
Critchell, K., Hoogenboom, M.O., 2018. Effects of microplastic exposure on the body condition and behaviour of planktivorous reef fish (*Acanthochromis polyacanthus*). PLoS One 13, e0193308.
Critchell, K., Lambrechts, J., 2016. Modelling accumulation of marine plastics in the coastal zone; what are the dominant physical processes?. Estuar. Coast. Shelf Sci. 171, 111–122.
Dai, A., Trenberth, K.E., 2002. Estimates of freshwater discharge from continents: Latitudinal and seasonal variations. J. Hydrometeorol. 3, 660–687.
Das, P., Marchesiello, P., Middleton, J.H., 2000. Numerical modelling of tide-induced residual circulation in Sydney Harbour. Mar. Freshw. Res. 51, 97–112.
de Silva Samarasinghe, J.R., 1989. Transient salt-wedges in a tidal gulf: A criterion for their formation. Estuar. Coast. Shelf Sci. 28, 129–148.
de Silva Samarasinghe, J.R., Lennon, G.W., 1987. Hypersalinity, flushing and transient salt-wedges in a tidal gulf—an inverse estuary. Estuar. Coast. Shelf Sci. 24, 483–498.
de Stephanis, R., Giménez, J., Carpinelli, E., Gutierrez-Exposito, C., Cañadas, A., 2013. As main meal for sperm whales: Plastics debris. Mar. Pollut. Bull. 69, 206–214.
Deleersnijder, E., Beckers, J.-M., Delhez, E.J.M., 2006. On the behaviour of the residence time at the bottom of the mixed layer. Environ. Fluid Mech. 6, 541–547.
Djamhur, M., Mennofatria, B., Bengen, D.G., Fachrudin, A., 2014. Assessments on development of ecotourist in Weda Bay, North Maluku province (in Indonesian language). Tata-Loka 16, 70–83.
Edinger, E.N., Jompa, J., Limmon, G.V., Widjatmoko, W., Risk, M.J., 1998. Reef degradation and coral biodiversity in Indonesia: effects of land-based pollution, destructive fishing practices and changes over time. Mar. Pollut. Bull. 36, 617–630.
Edinger, E.N., Kolasa, J., Risk, M.J., 2000. Biogeographic variation in coral species diversity on coral reefs in three regions of Indonesia. Divers. Distrib. 6, 113–127.
Elliott, M., Whitfield, A.K., 2011. Challenging paradigms in estuarine ecology and management. Estuar. Coast. Shelf Sci. 94, 306–314.
Evans, S.M., Dawson, M., Day, J., Frid, C.L.J., Gill, M.E., Pattisina, L.A., Porter, J., 1995. Domestic waste and TBT pollution in coastal areas of Ambon Island (Eastern Indonesia). Mar. Pollut. Bull. 30, 109–115.
Fabricius, K.E., 2005. Effects of terrestrial runoff on the ecology of corals and coral reefs: review and synthesis. Mar. Pollut. Bull. 50, 125–146.
Farmer, D.M., Freeland, H.J., 1983. The physical oceanography of Fjords. Prog. Oceanogr. 12, 147–219.
Ffield, A., Gordon, A.L., 1992. Vertical mixing in the Indonesian thermocline. J. Phys. Oceanogr. 22, 184–195.
Fok, L., Cheung, P.K., 2015. Hong Kong at the Pearl River Estuary: A hotspot of microplastic pollution. Mar. Pollut. Bull. 99, 112–118.
Geyer, W., 2010. Estuarine salinity structure and circulation. Contemp. Issues Estuar. Phys. 12–26.
Gómez, A., García Alba, J., Puente, A., Juanes, J., 2014. Environmental risk assessment of dredging processes–application to marin harbour (NW Spain). Adv. Geosci. 39, 101–106.
Gómez, A.G., Ondiviela, B., Puente, A., Juanes, J.A., 2015. Environmental risk assessment of water quality in harbor areas: A new methodology applied to European ports. J. Environ. Manag. 155, 77–88.
Good, T.P., June, J.A., Etnier, M.A., Broadhurst, G., 2010. Derelict fishing nets in Puget Sound and the Northwest Straits: patterns and threats to marine fauna. Mar. Pollut. Bull. 60, 39–50.
Guo, W., Wu, G., Liang, B., Xu, T., Chen, X., Yang, Z., Xie, M., Jiang, M., 2016. The influence of surface wave on water exchange in the Bohai Sea. Cont. Shelf Res. 118, 128–142.
Hamzah, M., Wenno, L.F., 1987. Ocean circulation of Ambon Bay (in Indonesian language). In: Soemodihardjo, S., Birowo, S., Romimohta, K. (Eds.), Teluk Ambon, Biologi, Perikanan, Oseanografi, Dan Geologi. In: Balai Penelitian dan Pengembangan Sumberdaya Laut, LIPI Ambon, Ambon, pp. 91–101.
Hancock, G.J., 2006. Horizontal mixing of Great Barrier Reef waters: Offshore diffusivity determined from radium isotope distribution. J. Geophys. Res. C Oceans 111.
Herdiansyah, H., Saiya, H.G., Afkarina, K.I.I., Indra, T.L., 2021. Coastal community perspective, waste density, and spatial area toward sustainable waste management (case study: Ambon bay, Indonesia). Sustainability 13, 10947.
Hermawan, R., Damar, A., Hariyadi, S., 2017. Daily accumulation and impacts of marine litter on the shores of Selayar Island Coast, South Sulawesi. Waste Technol. 5, 15–20.
Herzke, D., Ghaffari, P., Sundet, J.H., Tranang, C.A., Halsband, C., 2021. Microplastic fiber emissions from wastewater effluents: Abundance, transport behavior and exposure risk for Biota in an Arctic Fjord. Front. Environ. Sci. 9, 194.
Hoeksema, B., Hermanto, B., 2018. Plastic nets as substrate for reef corals in Lembeh Strait, Indonesia. Coral Reefs 37, 631.
Hope, B.K., 2006. An examination of ecological risk assessment and management practices. Environ. Int. 32, 983–995.
Hutubessy, B., Mosse, J.W., 2023. Identifying fish assemblages in tropical lagoon ecosystem: First record from luang island, South-west Maluku Indonesia. Aquac. Fish. 8, 221–226.
Indonesian Bureau of Statistics, 1980. 1980 Census Report. Indonesian Bureau of Statistics (BPS), Ambon.
Indonesian Bureau of Statistics, 2010. 2010 Census Report: Aggregated Data Per District of Ambon City. Indonesian Bureau of Statistics (BPS), Ambon, p. 9.
Ismail, F., Akbar, N., Tahir, I., Paembonan, R., Marus, I., Wibowo, E., 2021. An Assessment of Small IslandS Coral Cover and Coral-Reef Fish Diversity at Oba Sub-District, Halmahera Island. In: IOP Conference Series: Earth and Environmental Science, IOP Publishing, 012060.
Jakacki, J., Przyborska, A., Kosecki, S., Sundfjord, A., Albretsen, J., 2017. Modelling of the Svalbard fjord Hornsund. Oceanologia 59, 473–495.
Jambeck, J.R., Geyer, R., Wilcox, C., Siegler, T.R., Perryman, M., Andrady, A., Narayan, R., Law, K.L., 2015. Plastic waste inputs from land into the ocean. Science 347, 768.
Jorge, M.M., Miguel, F.L., Alejandro, F.P.-S., 2016. Seasonal heat and salt balance in the Upper Gulf of California. J. Coast. Res. 32, 853–862.
Josey, S.A., Kent, E.C., Taylor, P.K., 1998. The southampton oceanography centre (SOC) ocean-atmosphere heat, momentum and freshwater flux atlas.
Kakisina, T.J., Anggoro, S., Hartoko, A., Suripin, 2015. Analysis of the impact of land use on the degradation of coastal areas at Ambon Bay-mollucas Province Indonesia. Procedia Environ. Sci. 23, 266–273.
Kämpf, J., Ellis, H., 2015. Hydrodynamics and flushing of Coffin Bay, South Australia: A small tidal inverse estuary of interconnected bays. J. Coast. Res. 31, 447–456.
Kämpf, J., Payne, N., Malthouse, P., 2010. Marine connectivity in a large Inverse Estuary. J. Coast. Res. 1047–1056.
Karlsson, S., Nordén, A., 2018. Optimizingthe Placement of Cleanup Systems for Marine Plastic Debris : Amulti-Objective Approach. TRITA-SCI-GRU.
Lavın, M.F., Godınez, V.M., Alvarez, L.G., 1998. Inverse-estuarine features of the Upper Gulf of California. Estuar. Coast. Shelf Sci. 47, 769–795.
Lavín, M.F., Marinone, S.G., 2003. An overview of the physical oceanography of the Gulf of California. In: Velasco Fuentes, O.U., Sheinbaum, J., Ochoa, J. (Eds.), Nonlinear Processes in Geophysical Fluid Dynamics: A Tribute to the Scientific Work of Pedro Ripa. Springer Netherlands, Dordrecht, pp. 173–204.
Law, K.L., Morét-Ferguson, S., Maximenko, N.A., Proskurowski, G., Peacock, E.E., Hafner, J., Reddy, C.M., 2010. Plastic accumulation in the North Atlantic Subtropical Gyre. Science 329, 1185.

Lebreton, L.C., Van der Zwet, J., Damsteeg, J.-W., Slat, B., Andrady, A., Reisser, J., 2017. River plastic emissions to the world's oceans. Nature Commun. 8, 15611.

Li, W.C., Tse, H., Fok, L., 2016. Plastic waste in the marine environment: A review of sources, occurrence and effects. Sci. Total Environ. 566, 333–349.

Li, Y., Wolanski, E., Dai, Z., Lambrechts, J., Tang, C., Zhang, H., 2018. Trapping of plastics in semi-enclosed seas: Insights from the Bohai Sea, China. Mar. Pollut. Bull. 137, 509–517.

Li, Y., Wolanski, E., Zhang, H., 2015. What processes control the net currents through shallow straits? A review with application to the Bohai Strait, China. Estuar. Coast. Shelf Sci. 158, 1–11.

Limmon, G.V., Haulussy, Z., Loupatty, S.R., Manuputty, G.D., 2023. Corals Diversity At Waters of Southern Ambon Island, Maluku. In: AIP Conference Proceedings, AIP Publishing LLC, 030008.

Limmon, G., Manuputty, G., 2021. Coral Reef Condition at North Coastal of Haruku Island Maluku Tengah. In: IOP Conference Series: Earth and Environmental Science, IOP Publishing, 012042.

Lithner, D., Larsson, Å., Dave, G., 2011. Environmental and health hazard ranking and assessment of plastic polymers based on chemical composition. Sci. Total Environ. 409, 3309–3324.

Mahoney, T., 2017. The concentration of microplastics compared to relative population proximity and basin residence times. In: Hood Canal and Whidbey Basin in Puget Sound, WA. School of Oceanography University of Washington, Seattle, WA.

Mangubhai, S., Erdmann, M.V., Wilson, J.R., Huffard, C.L., Ballamu, F., Hidayat, N.I., Hitipeuw, C., Lazuardi, M.E., Pada, D., Purba, G., 2012. Papuan Bird's Head Seascape: Emerging threats and challenges in the global center of marine biodiversity. Mar. Pollut. Bull. 64, 2279–2295.

Manullang, C., 2019. The Abundance of Plastic Marine Debris on Beaches in Ambon Bay. In: IOP Conference Series: Earth and Environmental Science, IOP Publishing, 012037.

Manullang, C.Y., Barends, W., Polnaya, D., Soamole, A., Rehalat, I., 2021. Marine litter and grading of the coastal areas of Ambon Bay, Indonesia. Omni-Akuatika 17, 70–77.

Mao, Y., Ridd, P.V., 2015. Sea surface temperature as a tracer to estimate cross-shelf turbulent diffusivity and flushing time in the Great Barrier Reef lagoon. J. Geophys. Res.: Oceans 120, 4487–4502.

Mazarrasa, I., Puente, A., Núñez, P., García, A., Abascal, A.J., Juanes, J.A., 2019. Assessing the risk of marine litter accumulation in estuarine habitats. Mar. Pollut. Bull. 144, 117–128.

McLusky, D.S., Elliott, M., 2004. The Estuarine Ecosystem: Ecology, Threats and Management. OUP Oxford.

McManus, J.W., Wenno, J.J., 1981. Coral communities of outer ambon bay: a general assessment survey. Bull. Mar. Sci. 31, 574–580.

Monismith, S.G., Kimmerer, W., Burau, J.R., Stacey, M.T., 2002. Structure and flow-induced variability of the subtidal salinity field in Northern San Francisco Bay. J. Phys. Oceanogr. 32, 3003–3019.

Mudjiono, 2009. Continuing Ambon Bay Monitoring (in Indonesian Language). Annual report of 2009 Ambon Bay Monitoring Project, p. 91.

Murtiono, L.H., Anggoro, S., Sasongko, D.P., 2015. Assessment of the Effects of Aquaculture Activities on the Water Quality of Inner Ambon Bay (in Indonesian). Seminar Nasional IiEM, Universitas Diponegoro, Semarang.

Nahas, E.L., Pattiaratchi, C.B., Ivey, G.N., 2005. Processes controlling the position of frontal systems in Shark Bay, Western Australia. Estuar. Coast. Shelf Sci. 65, 463–474.

National Research Council, 1975. Assessing Potential Ocean Pollutants: A Report of the Study Panel on Assessing Potential Ocean Pollutants To the Ocean Affairs Board. Commission on Natural Resources, National Research Council. National Academy of Sciences.

Notanubun, R., Mussadun, M., 2017. A study on waterfront city plan in the coastal area of Ambon City (in Indonesian). J. Pembang. Wil. Dan Kota 13, 243–255.

Nurhayati, 2006. Vertical distribution of temperature, salinity and ocean currents in Morotai waters, North Maluku (in Indonesian). Oseanol. Limnol. Indones. 40, 29–41.

Ocean Conservancy, 2017. Stemming the Tide: Land-Based Strategies for a Plastic-Free Ocean. McKinsey Center for Business and Environment, p. 48.

Panti, C., Baini, M., Lusher, A., Hernandez-Milan, G., Bravo Rebolledo, E.L., Unger, B., Syberg, K., Simmonds, M.P., Fossi, M.C., 2019. Marine litter: One of the major threats for marine mammals, outcomes from the European Cetacean Society workshop. Environ. Pollut. 247, 72–79.

Pelasula, D., 2008. Impact of Deforestation on Upper Land To Marine Coastal Ecosystem on Ambon Bay (in Indonesian). Faculty of Fishery and Marine Sciences. Universitas Pattimura, Ambon, p. 103.

Pelasula, D., Manullang, C., Patria, M., Wouthuyzen, S., Lekallete, J., Malik, S., 2022. Destruction Level on Coral Reef in the Ambon Bay. In: IOP Conference Series: Earth and Environmental Science, IOP Publishing, 012077.

Pello, F.S., Adiwilaga, E.M., Huliselan, N.V., Damar, A., 2014. Effect of seasonal on nutrient load input the inner Ambon Bay. Bumi Lestari J. Environ. 14, 63–73.

PlasticEurope, 2015. Plastics - the Facts 2015: An Analysis of European Plastics Production, Demand and Waste Data. PlasticsEurope Market Research Group, Brussels.

Potere, D., 2008. Horizontal positional accuracy of Google Earth's high-resolution imagery archive. Sensors 8, 7973–7981.

Purba, N.P., Faizal, I., Pangestu, I.F., Mulyani, P.G., Fadhillah, M.F., 2018. Overview of physical oceanographic condition at Biawak Island: past achievement and future challenge. IOP Conference Series: Earth and Environmental Science 176, 012001.

Putri, M.R., Mudjiono, Basit, A., 2008. Monitoring of Physical Oceanography in Ambon Bay (in Indonesian Language). In: Indonesian Oceanologist Conference, Indonesian Institute of Sciences (LIPI), pp. 41–47.

Putri, M.R., Pohlmann, T., 2009. Hydrodynamic and transport model of the Siak Estuary. Asian J. Water Environ. Pollut. 6, 67–80.

Radjawane, I., Riandini, F., 2010. Numerical simulation of cohesive sediment transport in Jakarta Bay. Int. J. Remote Sens. Earth Sci. (IJReSES) 6.

Rochman, C.M., Browne, M.A., Halpern, B.S., Hentschel, B.T., Hoh, E., Karapanagioti, H.K., Rios-Mendoza, L.M., Takada, H., Teh, S., Thompson, R.C., 2013. Classify plastic waste as hazardous. Nature 494, 169–171.

Sahetapy, D., Limmon, G., Tetelepta, J., Pattikawa, J., Rijoly, F., Masrikat, J., Loupatty, S., 2021. Coral Reef Condition in the Coastal Waters of Kei Besar Island, Southeast Maluku-Indonesia. In: IOP Conference Series: Earth and Environmental Science, IOP Publishing, 012002.

Sahetapy, D., Retraubun, A., Bengen, D., Abrahamsz, J., 2018. Coral reef fishes of Tuhaha Bay, Saparua Island, Maluku province, Indonesia. Int. J. Fish. Aquat. Stud. 6, 105–109.

Salamena, G.G., 2010. Monitoring the Physical Properties of Ambon Bay in 2010 (in Indonesian Language). Annual Report of 2010 Ambon Bay Monitoring Project., LIPI Marine Lab, Ambon.

Salamena, G.G., 2011. Monitoring the Physical Properties of Ambon Bay in 2011 (in Indonesian Language). Annual Report of 2011 Ambon Bay Monitoring Project, LIPI Marine Lab, Ambon.

Salamena, G.G., 2012. Monitoring the Physical Properties of Ambon Bay in 2012 (in Indonesian Language). Annual Report of 2012 Ambon Bay Monitoring Project, LIPI Marine Lab Ambon.

Salamena, G.G., Martins, F., Ridd, P.V., 2016. The density-driven circulation of the coastal hypersaline system of the Great Barrier Reef, Australia. Mar. Pollut. Bull. 105, 277–285.

Salamena, G.G., Whinney, J.C., Heron, S.F., 2022a. Vertical circulation due to deep-water renewal and phytoplankton blooms in the tropical fjord of Ambon Bay, eastern Indonesia. J. Mar. Syst. 234, 103776.

Salamena, G.G., Whinney, J.C., Heron, S.F., Ridd, P.V., 2021. Internal tidal waves and deep-water renewal in a tropical fjord: lessons from Ambon Bay, eastern Indonesia. Estuar. Coast. Shelf Sci. 253, 107291.

Salamena, G.G., Whinney, J.C., Heron, S.F., Ridd, P.V., 2022b. Frontogenesis and estuarine circulation at the shallow sill of a tropical fjord: Insights from Ambon Bay, eastern Indonesia. Reg. Stud. Mar. Sci. 56, 102696.

Sapulete, D., 1996. Vertical profiles of temperature and salinity in relation to potential upwelling in Piru Bay (in Indonesian language). Perair. Maluku Sekitarnya 11, 139–148.

Sheehan, E., Rees, A., Bridger, D., Williams, T., Hall-Spencer, J., 2017. Strandings of NE atlantic gorgonians. Biol. Cons. 209, 482–487.

Siahaya, W.A., 2016. The Effects of Changes in Land Cover on Changes in Coastal Benthic Cover of Small Island Based on the Analysis of Medium Resolution Satellite Image (the Case Study of Fourteen River Catchment Disharging Into Ambon Bay) (Indonesian Language). Department of Remote Sensing. Universitas Gadjah Mada, Yogyakarta, Indonesia, p. 275.

Soto-Navarro, J., Jordá, G., Deudero, S., Alomar, C., Amores, Á., Compa, M., 2020. 3D hotspots of marine litter in the Mediterranean: a modeling study. Mar. Pollut. Bull. 155, 111159.

Souisa, M., Hendrajaya, L., Handayani, G., 2016. LandSlide Hazard and Risk Assessment for Ambon City using LandSlide Inventory and Geographic Information System. In: Journal of Physics: Conference Series, IOP Publishing, 012078.

Stanley, G.D., 2006. Photosymbiosis and the evolution of modern coral reefs. Science 312, 857.

Stigebrandt, A., Aure, J., 1989. Vertical mixing in basin waters of Fjords. J. Phys. Oceanogr. 19, 917–926.

Suedel, B.C., Kim, J., Clarke, D.G., Linkov, I., 2008. A risk-informed decision framework for setting environmental windows for dredging projects. Sci. Total Environ. 403, 1–11.

Suyadi, Manullang, C.Y., 2020. Distribution of plastic debris pollution and it is implications on mangrove vegetation. Mar. Pollut. Bull. 160, 111642.

Swaney, D.P., Smith, S.V., Wulff, F., 2011. 9.08 - The LOICZ biogeochemical modeling protocol and its application to estuarine ecosystems. In: Wolanski, E., McLusky, D. (Eds.), Treatise on Estuarine and Coastal Science. Academic Press, Waltham, pp. 135–159.

Syahailatua, A., Wouthuyzen, S., Pelasula, D.D., 2012. Coral Reefs in Ambon Bay Need Sustainable Management: Insights from 40 Years of Monitoring. RIN Dataverse.
Tanner, E.L., Mulhearn, P.J., Eyre, B.D., 2017. CO2 emissions from a temperate drowned river valley estuary adjacent to an emerging megacity (Sydney Harbour). Estuar. Coast. Shelf Sci. 192, 42–56.
Tarigan, M.S., Wenno, L.F., 1991. Upwelling in Ambon Bay (in Indonesian language). Perair. Maluku Sekitarnya 2.
Tett, P., Portilla, E., Gillibrand, P.A., Inall, M., 2011. Carrying and assimilative capacities: the ACExR-LESV model for sea-loch aquaculture. Aquac. Res. 42, 51–67.
Umar, M., McCook, L., Price, I., 1998. Effects of sediment deposition on the seaweed Sargassum on a fringing coral reef. Coral Reefs 17, 169–177.
UN Environment, 2017. Marine Litter: Socio Economic Study. United Nations Environment Programme, Nairobi, Kenya, p. 144.
Uneputty, P., Evans, S.M., 1997a. The impact of plastic debris on the biota of tidal flats in Ambon Bay (eastern Indonesia). Mar. Environ. Res. 44, 233–242.
Uneputty, P.A., Evans, S.M., 1997b. Accumulation of beach litter on islands of the Pulau Seribu Archipelago, Indonesia. Mar. Pollut. Bull. 34, 652–655.
Uneputty, P., Evans, S., Suyoso, E., 1998. The effectiveness of a community education programme in reducing litter pollution on shores of Ambon Bay (eastern Indonesia). J. Biol. Educ. 32, 143–147.
van der Wulp, S.A., Damar, A., Ladwig, N., Hesse, K.-J., 2016. Numerical simulations of river discharges, nutrient flux and nutrient dispersal in Jakarta Bay, Indonesia. Mar. Pollut. Bull. 110, 675–685.
Vegter, A.C., Barletta, M., Beck, C., Borrero, J., Burton, H., Campbell, M.L., Costa, M.F., Eriksen, M., Eriksson, C., Estrades, A., Gilardi, K.V.K., Hardesty, B.D., Ivar do Sul, J.A., Lavers, J.L., Lazar, B., Lebreton, L., Nichols, W.J., Ribic, C.A., Ryan, P.G., Schuyler, Q.A., Smith, S.D.A., Takada, H., Townsend, K.A., Wabnitz, C.C.C., Wilcox, C., Young, L.C., Hamann, M., 2014. Global research priorities to mitigate plastic pollution impacts on marine wildlife. Endanger. Species Res. 25, 225–247.
Vélez-Rubio, G.M., Estrades, A., Fallabrino, A., Tomás, J., 2013. Marine turtle threats in Uruguayan waters: insights from 12 years of stranding data. Mar. Biol. 160, 2797–2811.
Veron, J., Devantier, L.M., Turak, E., Green, A.L., Kininmonth, S., Stafford-Smith, M., Peterson, N., 2009. Delineating the coral triangle, Galaxea. J. Coral Reef Stud. 11, 91–100.
Veron, J.C.E., DeVantier, L.M., Turak, E., Green, A.L., Kininmonth, S., Stafford-Smith, M., Peterson, N., 2011. The Coral Triangle, Coral Reefs: An Ecosystem in Transition. Springer, pp. 47–55.
Wang, Y., Ridd, P.V., Heron, M.L., Stieglitz, T.C., Orpin, A.R., 2007. Flushing time of solutes and pollutants in the central Great Barrier Reef lagoon, Australia. Mar. Freshw. Res. 58, 778–791.
Wattimena, M.C., Salamena, G.G., 2022. Characteristics of surface winds over Ambon Bay, Maluku (in Indonesian). J. Laut Pulau: Hasil Penelit. Kelaut. 1, 19–36.
Wattimena, M.C., Supusepa, J., Lokollo, F.F., Krisye, K., Ratuluhain, E.S., Tuahatu, J.W., Kesaulya, I., Tubalawony, S., Saleky, V.D., Fakaubun, F.R., 2023. The improvement Of Coastal environment quality through beach clean-up program in Rumah Tiga Village, Ambon City (in Indonesian). MESTAKA: J. Pengabdi. Kpd. Masy. 2, 104–108.
Waworuntu, J.M., Fine, R.A., Olson, D.B., Gordon, A.L., 2000. Recipe for Banda Sea water. J. Mar. Res. 58, 547–569.
Wenno, L.F., Anderson, J.J., 1984. Evidence for tidal upwelling across the sill of Ambon Bay. Mar. Res. Indones. 23, 13–20.
Wilcox, C., Puckridge, M., Schuyler, Q.A., Townsend, K., Hardesty, B.D., 2018. A quantitative analysis linking sea turtle mortality and plastic debris ingestion. Sci. Rep. 8, 12536.
Willoughby, N.G., Sangkoyo, H., Lakaseru, B.O., 1997. Beach litter: an increasing and changing problem for Indonesia. Mar. Pollut. Bull. 34, 469–478.
World Bank Group, 2018. Indonesia Marine Debris Hotspot: Rapid Assessment. World Bank, p. 42.
Xu, Q., Zheng, J., 1991. Environmental management of the Bohai Sea in China. Mar. Pollut. Bull. 23, 573–578.
Yu, L., 2007. Global variations in oceanic evaporation (1958–2005): The role of the changing wind speed. J. Clim. 20, 5376–5390.
Zhang, L., Liu, J., Xie, Y., Zhong, S., Yang, B., Lu, D., Zhong, Q., 2020. Distribution of microplastics in surface water and sediments of Qin river in Beibu Gulf, China. Sci. Total Environ. 708, 135176.
Zhang, W., Zhang, S., Wang, J., Wang, Y., Mu, J., Wang, P., Lin, X., Ma, D., 2017. Microplastic pollution in the surface waters of the Bohai Sea, China. Environ. Pollut. 231, 541–548.
Zhu, X., Ran, W., Teng, J., Zhang, C., Zhang, W., Hou, C., Zhao, J., Qi, X., Wang, Q., 2020. Microplastic pollution in nearshore sediment from the Bohai Sea Coastline. Bull. Environ. Contam. Toxicol. 1–6.
Zhu, J., Zhang, Q., Huang, Y., Jiang, Y., Li, J., Michal, J.J., Jiang, Z., Xu, Y., Lan, W., 2021. Long-term trends of microplastics in seawater and farmed oysters in the Maowei Sea, China. Environ. Pollut. 273, 116450.
Zhu, J., Zhang, Q., Li, Y., Tan, S., Kang, Z., Yu, X., Lan, W., Cai, L., Wang, J., Shi, H., 2019. Microplastic pollution in the Maowei Sea, a typical mariculture bay of China. Sci. Total Environ. 658, 62–68.